Wefer, G., Berger, W.H., and Richter, C. (Eds.)
Proceedings of the Ocean Drilling Program, Scientific Results Volume 175

11. Siliceous Phytoplankton Productivity Fluctuations in the Congo Basin over the Past 460,000 Years: Marine vs. Riverine Influence, ODP Site 1077[1]

E. Uliana,[2] C.B. Lange,[3] B. Donner,[2] and G. Wefer[2]

ABSTRACT

Accumulation rates, concentrations, and relative abundance of siliceous microfossils from Site 1077 are used to reconstruct changes in marine productivity and climate history of the Congo Fan area. The major contributors to siliceous productivity are marine diatoms, which show highest concentrations during glacial stages and cooler substages of the last interglacial. Abrupt changes are observed during Termination II (oxygen isotope Stage 5/6 boundary): (1) the marine diatom signal varies in amplitude and assemblage composition from predominantly marine to marine/brackish and (2) the environmental setting on land obtained from freshwater diatoms and chrysophycean cysts points to changes from more arid conditions accompanied by a large drainage area of the Congo River to more humid conditions and a decrease in the inland water content for the last 125 k.y.

INTRODUCTION

During Ocean Drilling Program (ODP) Leg 175, the Lower Congo Basin (LCB) off west Africa was the target for three drilling sites (1075, 1076, and 1077) along a transect on the northern rim of the Congo Fan (Shipboard Scientific Party, 1998a). Here, one of the largest rivers in terms of freshwater discharge joins an oceanic high-fertility area. The

[1]Uliana, E., Lange, C.B., Donner, B., and Wefer, G., 2001. Siliceous phytoplankton productivity fluctuations in the Congo Basin over the past 460,000 years: marine vs. riverine influence, ODP Site 1077. *In* Wefer, G., Berger, W.H., and Richter, C. (Eds.), *Proc. ODP, Sci. Results,* 175, 1–32 [Online]. Available from World Wide Web: <http://www-odp.tamu.edu/publications/175_SR/VOLUME/CHAPTERS/SR175_11.PDF>. [Cited YYYY-MM-DD]
[2]Fachbereich Geowissenschaften, Klagenfurter Strasse, Universität Bremen, 28359 Bremen, Federal Republic of Germany. Correspondence author: **eleonora@uni-bremen.de**
[3]Scripps Institution of Oceanography, University of California at San Diego, Geosciences Research Division, La Jolla CA 92093-0244, USA.

Initial receipt: 7 March 2000
Accepted: 14 September 2000
Web publication: 26 April 2001
Ms 175SR-216

regional environment is dominated by seasonal coastal upwelling and associated filaments and eddies moving offshore, by riverine input from the Congo River, and by incursions of open-ocean waters, especially from the South Equatorial Countercurrent (Fig. F1). Thus, the combination of pelagic and terrigenous information contained in these fan-margin deposits provides an excellent opportunity for studying simultaneous climatic changes on land and sea.

One of the goals of Leg 175 included the reconstruction of the history of productivity off Angola and Namibia and the influence of the Congo River, thereby extending available information about the late Quaternary (e.g., Schneider et al., 1994, 1996, 1997; Jansen et al., 1996, and references therein) to earlier periods (Shipboard Scientific Party, 1998a). According to Jansen (1985), river-induced phytoplankton activity extends ~160 km beyond the shelf edge and would affect all three sites drilled. However, it is also evident from these earlier studies that major productivity changes off the Congo are determined by wind forcing and oceanic subsurface nutrient supply rather than merely reflecting fertility changes induced by river discharge of nutrients. In an elegant work using oxygen and carbon isotope data of two planktonic foraminifers, Schneider et al. (1994) showed that off the Congo, ocean dynamics have overwhelmed the influence of one of the world's largest rivers on marine coastal productivity over the past 190 k.y. This is contrary to other areas off major rivers where a strong freshwater signal was described (Pastouret et al., 1978; Showers and Bevis, 1988).

High opal content characterizes the Congo Fan sediments (Müller and Schneider, 1993) where diatoms dominate. Schneider et al. (1997) suggested that enhanced opal production in this region was the result of additional fluvial supply of dissolved silica during humid climates characterized by more intense chemical weathering on the continent, whereas total paleoproductivity created by oceanic upwelling was high in periods of increased zonal trade wind intensity at precessional insolation minima and during cold, more arid glacial climate conditions.

Here, we present a record of siliceous microfossil paleoproductivity spanning the last 460 k.y. from upper Pleistocene sediments of ODP Site 1077. By using accumulation rates and the relative contribution of siliceous components of both continental origin (freshwater diatoms, phytoliths, and chrysophycean cysts) and marine origin (marine diatoms, silicoflagellates, and radiolarians) in combination with organic matter and opal data from nearby sites (ODP Site 1075 and GeoB1008), we aim to reconstruct temporal fluctuations in the Congo River freshwater outflow, coastal upwelling, and open-ocean contributions to the dynamics of the region. Our findings are integrated with and compared to those of previous studies from nearby sites in the Congo Fan and off Angola (e.g., Mikkelsen, 1984; Jansen et al., 1984; van Iperen et al., 1987; Jansen and van Iperen, 1991; Schneider et al., 1994, 1995, 1997; Gingele et al., 1998).

F1. Location of Sites 1077, 1075, and GeoB1008 and main surface and subsurface currents in the eastern Angola Basin, p. 17.

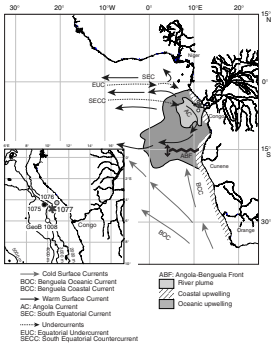

REGIONAL SETTING

Hydrography

Detailed studies of modern hydrography in the eastern Angola Basin and the Congo Fan area are given by Eisma and van Bennekom (1978), van Bennekom and Berger (1984), and Schneider et al. (1995). The com-

plex hydrography of the area involves different water masses with characteristic physical and biological properties.

In the eastern Angola Basin (0°–20°S), the surface and shallow subsurface circulation is dominated by the Angola Current (AC) and the Benguela Coastal Current (BCC). The AC flows southward along the African coast and is fed by the eastward-flowing, shallow-subsurface warm South Equatorial Countercurrent (SECC). The BCC transports cold, nutrient-rich waters northward across Walvis Ridge. The two currents converge between 14°S and 16°S, depending on the season, and form the Angola Benguela Front (ABF) (Fig. F1). In a zone between 10°S and 16°S, the interaction between the SECC, AC, and BCC creates a complicated pattern of fronts, gyres, and thermal domes (e.g., Angola Dome), bringing nutrient-rich shallow subsurface waters into the euphotic zone (oceanic upwelling). North of the ABF, the BCC can be traced as a shallow subsurface current to 5°S (van Bennekom and Berger, 1984). The ABF delineates the northern boundary of the zonally directed tradewind field. North of the ABF, winds weaken and change to a meridional direction (summary in Schneider et al., 1995). Coastal upwelling is restricted to two narrow areas north and south of the Congo estuary and is considered to be the result of upwelling of colder waters of the Equatorial Undercurrent.

Superimposed on the system described above is the influence of the Congo River and fan area, which supplies freshwater, nutrients (including large amounts of dissolved SiO_2), and sediments to the ocean. The Congo River is the second largest river in the world. It has a peculiar estuarine hydrography caused by the small river mouth, which includes the canyon head (Jansen, 1984). This forces a rapid outflow of river water toward the ocean in a sharply bounded turbid surface layer 5–15 m thick, which also entrains subsurface oceanic waters rich in phosphate and nitrate (Eisma and van Bennekom, 1978). The plume of Congo water, characterized by reduced surface-water salinity, can be detected as far as 800 km offshore during austral summer, when monsoonal circulation and precipitation reach their maximum seasonal intensity (Eisma and van Bennekom, 1978; van Bennekom and Berger, 1984). Salinity is <30‰ in the inner plume area. Farther offshore (150–200 km from the river mouth), the plume broadens, salinity rises to ~30‰, and maxima in primary production (river-induced upwelling) (van Bennekom and Berger, 1984), diatom cell numbers (Cadée, 1978, 1984), and diatom accumulation rates in the sediments (van Iperen et al., 1987) are found.

As a result of coastal, oceanic, and river-induced upwelling, modern primary productivity is very high in the surface waters off the Congo; Berger et al. (1989) gives values of 90–125 $gC/m^2/yr$. Data on biogenic silica production indicate high diatom productivity in the surface waters surrounding the central Congo plume, accounting for 40%–60% of the total carbon productivity (van Bennekom and Berger, 1984).

Sediments

Sedimentation within the LCB is dominated by rainout of suspended clay derived from the Congo River and by pelagic settling of biogenic debris. Since the Congo River drops most of its coarse load before reaching the ocean (unlike other river-influenced hemipelagic systems), LCB sediments lack a significant river-borne sand and silt fraction (Jansen et al., 1984). Wind-derived silt is minimal in relation to the amount of river-deposited clay (Jansen et al., 1984; van der Gaast and Jansen, 1984). Kaolinite and smectite are the most important clay minerals in

the surface sediments of the Congo Fan (van der Gaast and Jansen, 1984; Gingele et al., 1998). Other important terrigenous components include fresh- and brackish-water diatoms, plant remains, and phytoliths. The marine biogenic components include marine diatoms (dominating), coccoliths, planktonic and benthic foraminifers, silicoflagellates, radiolarians, dinoflagellate cysts, ebridians, and sponge spicules (e.g., Jansen et al., 1984; Mikkelsen, 1984; van Iperen et al., 1987; Jansen and van Iperen, 1991).

Site 1077 (5°10´S, 10°26´E) is the intermediate-water drill site on a depth transect in the LCB, located in 2382 m water depth at the northern edge of the Congo River plume (Fig. F1). Three holes (Holes 1077A, 1077B, and 1077C) were cored with the advanced hydraulic piston corer to a maximum depth of 205.1 meters below seafloor (mbsf), which recovered a continuous hemipelagic sedimentary section spanning the entire Pleistocene. Sediments are dominated by diatomaceous, partially carbonate-bearing clays (Shipboard Scientific Party, 1998c). Sedimentological evidence suggests that Site 1077 is not affected by turbidity currents (Pufahl et al., 1998). The sediment composition of ODP Site 1075 does not differ significantly from Site 1077 and consists entirely of greenish gray diatomaceous clay and nannofossil-bearing diatomaceous clay (Shipboard Scientific Party, 1998b.

MATERIALS AND METHODS

Siliceous Microfossils

We investigated samples from Site 1077. Sampling was mainly performed on Hole 1077A, although for some intervals additional samples were collected from Holes 1077B and 1077C. Meters below seafloor were transformed to meters composite depth (mcd) according to Shipboard Scientific Party (1998c).

High-resolution (20-cm sampling intervals) stable isotope analysis was performed on handpicked samples of the planktonic foraminifer *Globigerinoides ruber* (size >150 µm). A Finnigan MAT 251 micromass spectrometer equipped with a Kiel automated carbonate preparation device was used.

Samples (5 cm^3) were also collected for siliceous microfossil analysis. Sampling intervals varied from every 45 cm for the upper 44 mcd (representing an average resolution of ~2 k.y.) to every 110–120 cm downcore to 70 mcd; resolution for the lower part ranges from ~5 to 10 k.y. Samples were freeze-dried, and 0.4 g of dry sediment for each sample was treated with hydrochloric acid and hydrogen peroxide to dissolve carbonates and organic matter following the method of Schrader and Gersonde (1978); sodium pyrophosphate was added to remove clay-sized particles in suspension. Acid and salt remains were removed by repeated steps of rising with distilled water and settling. Preparation of slides for qualitative and quantitative analyses was performed according to Lange et al. (1994).

Identification and counting of taxa was done with a Zeiss-axioscope with phase-contrast illumination at 1000× magnification. Because of the overwhelming dominance of a few diatom taxa, the counting procedure was divided into two steps: (1) for the most abundant diatom species (e.g., *Thalassionema nitzschioides* var. *nitzschioides, Cyclotella litoralis,* and *Chaetoceros* spp.) just one transect across the slide was quantified; (2) for the rest of the diatom species, radiolarians, silicoflagellates,

ebridians, phytoliths, chrysophycean cysts, and the siliceous skeleton of the dinoflagellate *Actiniscus pentasterias,* a fraction of the slide (one-third, one-fifth, or one-tenth, depending on abundance) was counted. Sponge spicules were not included in our analysis. Definition of counting units followed that of Schrader and Gersonde (1978). Diatoms and silicoflagellates were identified to the lowest taxonomic level possible, whereas all other siliceous microfossils were counted as groups. Abundances of taxa and/or microfossil groups were calculated as concentrations per gram and as accumulation rates (AR). Relative abundances of individual species or group of species were calculated as percent of total assemblage. Accumulation rates for the different microfossils studied was calculated according to van Andel et al. (1975), as follows:

$$AR = \delta \times a \times SR,$$

where

- δ = dry bulk density in grams per cubic centimeter (obtained from **www-odp.tamu.edu/publications/175_IR/COREDATA/SITE1077/HOLE_A/GRAPE.DAT**);
- a = the estimated concentration for each group of siliceous microfossils per gram of sediment; and
- SR = sedimentation rates in centimeters per thousand years obtained by linear interpolation between isotopic tie points.

All data are available through the PANGAEA server (**www.pangaea.de/Projects/SFB261/EUliana_et_al_2000/**).

We used the PhFD Index introduced by Jansen et al. (1989) as an index of paleoaridity over equatorial Africa. This index is a ratio between the concentration of phytoliths and freshwater diatoms (Ph/[Ph+FD]). High values are related to arid conditions over the continent (higher abundance of phytoliths), whereas low values (high freshwater diatom concentrations) may reflect stronger river influence in the Congo area.

Biogenic Components

Biogenic opal content was measured on Site 1075 samples by Hui-Ling Lin at the National Sun Yat-Sen University of Taiwan. Opal contents were determined by the basic leaching method of Mortlock and Froelich (1989), modified by using different acid and base reagents (Lange et al., 1999; Lin et al., in press). Values reported here as opal contents are calculated (based on Mortlock and Froelich [1989]) as follows:

$$\text{Opal (wt\%)} = 2.4 \times \text{Si}_{\text{opal}} \text{ (wt\%)}$$

Total carbon and organic carbon (TOC) concentrations were measured on Site 1075 samples using a LECO CS-244 carbon/sulfur analyzer. Analytical details are given in Lin et al. (in press).

RESULTS

Oxygen Isotopes and Age Model

The $\delta^{18}O$ record of the planktonic foraminifer *G. ruber* (pink) from Site 1077 exhibits the shape typical for Quaternary records (Fig. F2), resulting from changes in seawater $\delta^{18}O$ due to the buildup and retreat of glacial polar ice caps and changes in water temperature (e.g., Shackleton and Opdyke, 1973; Schneider et al., 1996). The Holocene peak at 1.25 mcd was fixed as age control point 7 ka. It corresponds to the Climatic Optimum and also reflects increased discharge of isotopically light Congo River water. Pastouret et al. (1978) and Schneider et al. (1994) had already observed this variation superimposed on the classical $\delta^{18}O$ record of planktonic foraminifers in this area. All age control points used are listed in Table T1, and the age model is plotted in Figure F3. Features in the $\delta^{18}O$ data set of ODP Site 1077 were aligned with the record from Site 677 (Panama Basin) (Shackleton et al., 1990). For depth intervals with low carbonate content (between 60 and 95 mcd), the record of magnetic susceptibility was successfully used to (1) align the isotope record and (2) assign age-depth intervals (Dupont et al., 2000). The magnetostratigraphy corresponds well with the isotope record (Matuyama/Brunhes boundary; Stage 19).

Sedimentation Rates

Sedimentation rates were calculated by linear interpolation between age control points (Figs. F2, F4). Lowest values (8–11 cm/k.y.) correspond to glacial Stages 6, 10, and 12; highest values ranged between 17 and 22 cm/k.y. within Stages 11, 9, 8, and during the past 120 k.y. In Figure F2, we compare Site 1077 sedimentation rates during the last 200 k.y. with those from a well-studied core (GeoB1008) (Schneider, 1991) retrieved from 3124 m water depth just south of our site and located within the Congo River plume (GeoB1008; 6°35´S, 10°19´E; water depth = 3124 m). The shallower water depth at Site 1077 (2382 m) probably accounts for overall higher sedimentation rates. Discrepancies in the curve shapes (e.g., within Stages 5 and 6) may be attributed to local differences in sedimentation patterns and/or errors in age-depth alignment by correlation of individual $\delta^{18}O$ records to the SPECMAP standard stack.

Records of Biogenic Constituents

Organic Carbon

Only shipboard data are available for Site 1077 (Shipboard Scientific Party, 1998c). TOC values range from 1.9 to 4.7 wt% over the past 500 k.y. (Shipboard Scientific Party, 1998c). Higher resolution data do exist for core GeoB1008 (Schneider et al., 1997) and for nearby Site 1075 (4°47´S, 10°4.5´E; water depth = 2995 m) (Lin et al., in press). Both data sets are presented in Figure F2. Schneider et al. (1997) has shown that variations of TOC in the Congo Fan core GeoB1008 are mainly the result of changes in marine organic carbon (MOC) with values between 0.5 and 4 wt%. TOC concentrations at Site 1075 range from ~1.5 to 3.6 wt%. Here also, the organic matter appears to be mostly of marine origin (Shipboard Scientific Party, 1998b) and the relative contribution of terrestrial organic carbon is low (~0.5 wt%) (B. Jahn, pers. comm.,

F2. Comparison of Sites 1077 and 1075 with core GeoB1008, p. 18.

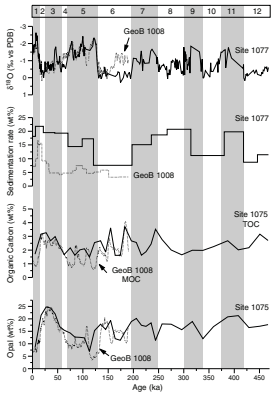

T1. Age model used at Site 1077, p. 25.

F3. Age model used at Site 1077 based on the planktonic foraminifer *Globigerinoides ruber* pink, p. 19.

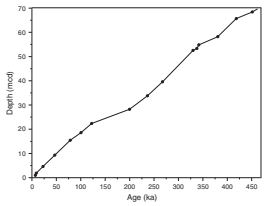

F4. Abundances of the most abundant siliceous microfossils counted, p. 20.

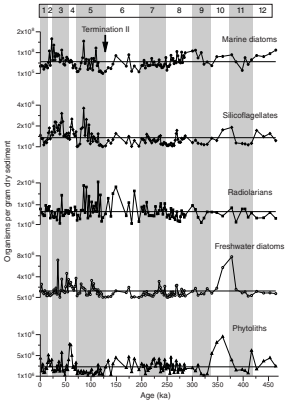

2000). It is evident that discrepancies in the timing of some peaks and valleys, especially during Stage 5, are due to (1) the very preliminary stratigraphy of Site 1075, which is based on shipboard nannofossil datum events (Shipboard Scientific Party, 1998b) and (2) differences in sampling strategy (every 5 cm for GeoB1008 and every ~1.5 m for Site 1075). However, the patterns are possibly comparable between both sites and higher percentages of MOC correspond to Stages 2 and 3 and to Substages 5.2, 5.4, 6.2, 6.4, and 6.6 (Fig. F2) (Schneider et al., 1994).

Biogenic Opal

Upper Quaternary Congo Fan sediments have high contents of biogenic silica (van der Gaast and Jansen, 1984; Schneider et al., 1997). In Figure F2, we plot two comparable records of biogenic silica for core GeoB1008 (Schneider, 1991) and Site 1075 (Lin et al., in press), both measured with automated wet leaching methods (Müller and Schneider, 1993, for GeoB1008; Mortlock and Froelich, 1989, for Site 1075). Values range from ~5 to 25 wt%. Although discrepancies in the timing of events over the last 200 k.y. are due to differences in sampling strategy and age model (see "Organic Carbon," p. 6), strong minima are observed in the Holocene and during the warmest period of the last interglacial (Substage 5.5 for core GeoB1008) and higher contents correspond to late Stage 3–early Stage 2, Substage 5.4, and within Stage 6.

For the older record (beyond the last 200 k.y.), the sample density of Site 1075 is too low and the age model is too preliminary to deduce accurate timing of changes in productivity based on TOC and opal fluctuations downcore. These preliminary data point to higher TOC values in late Stage 8–early Stage 7 and Stages 11 and 12. Obvious minima in opal weight percent correspond to Terminations 7/8 and 9/10.

Siliceous Organisms

Sediments of the Congo Fan area contain large amounts of siliceous microfossils. Only the dominant siliceous components are discussed below (in terms of accumulation rates, concentration, and species composition). Concentrations (per gram of dry sediment) of the most abundant microfossil groups counted are represented in Figure F5 and Table T2, and their accumulation rates are shown in Figure F4. The marine signal dominates at Site 1077, in agreement with previous studies (van Iperen et al., 1987; Jansen and van Iperen, 1991; Schneider et al., 1997). Abundances of marine diatoms are overwhelming (average = 5 × 10^7 valves/g); they compose 97% of the diatom assemblage (Table T3). The preservation state of the valves is moderate to good; lightly silicified species (e.g., vegetative cells and setae of *Chaetoceros*, *Bacteriastrum elongatum/furcatum,* and *Skeletonema costatum*) are present throughout. However, corroded valve edges were also observed (see also van Iperen et al., 1987). Silicoflagellates and radiolarians follow in second place, with abundances of 10^4–10^6 individuals/g dry sediment. For the three marine siliceous groups, concentrations tend to be higher (although highly variable) between 10 and 70 ka (especially for marine diatoms and silicoflagellates), during cooler conditions (Schneider et al., 1995) of Substages 5.2 and 5.4, and during glacial Stages 6 (especially for radiolarians), 8 and 9 (marine diatoms), and 10 and 12 (marine diatoms and silicoflagellates) (Fig. F5).

The continental signal is driven by freshwater diatoms with absolute abundances on the order of 10^6 valves/g (Fig. F5), an order of magni-

F5. Marine signal based on accumulation rates of marine organisms, p. 21.

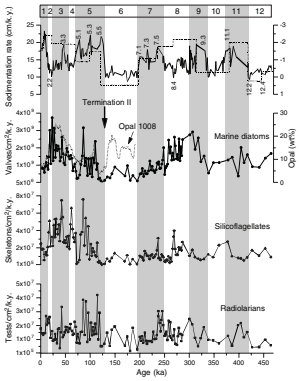

T2. Depth, density, sedimentation rate, and concentration of siliceous organisms, Site 1077, p. 26.

T3. Species composition and environmental conditions of diatom groups, Site 1077, p. 29.

tude lower than marine diatoms. They originate from the drainage area of the Congo River. Chrysophycean cysts and phytoliths are present in almost all samples. Chrysophycean cysts are siliceous resting stages of chrysophyceaen algae, which are commonly found in lakes (Smol, 1988); phytoliths are discrete, solid bodies of opaline silica in epidermal cells of grasses (Alexander et al., 1997; Runge, 1999). Phytolith concentrations average 10^5 bodies/g dry sediment, and accumulation rates are ~10^7 bodies/cm/k.y. The ratio of phytoliths to marine diatoms (×100) is low, 0.59, in agreement with the geographical distribution published by van Iperen et al. (1987). Phytolith maxima tend to coincide with glacial periods, whereas higher contributions of freshwater diatoms fall within interglacial stages (Fig. F5) and tend to occur during maxima in boreal summer insolation over Africa (Fig. F6). Both groups showed a significant difference in average concentration between glacial and interglacial times (Student's t test [Sokal and Rohlf, 1973]: T freshwater diatoms = 26.7, and T phytoliths = 4.8; with $t_{(0.05;\ 128)} = 2.626$). Values for the PhFD index (Jansen and van Iperen, 1991) average 0.2 and range between ~0 (almost no phytoliths) and 0.8 (reduced influx of freshwater diatoms to the sediments); they are comparable to Jansen and van Iperen's (1991) PhFD indices for nearby cores T78-3 (5°11´S, 7°58´E) and T78-46 (6°50´S, 10°45´E).

ARs were also calculated for each siliceous group. Although accumulation records are highly dependent on sedimentation rates (see discussion in Schneider et al., 1996), absolute abundances of each siliceous group are so high that they drive the AR pattern (cf. Figs. F5 and F4). ARs of marine diatoms range from 3.9 × 10^6 to 3.7 × 10^9 valves/cm/k.y. and are highest during Stage 2 and late Stage 3, Substages 5.2 and 5.4, Stage 8, and late Stage 9. Between 460 and 125 ka, silicoflagellate values oscillate around the mean (1.8 × 10^7 skeletons/cm/k.y.) and show an abrupt increase at ~100 ka with maxima at ~40, 60, and 85 ka (Fig. F4). Radiolarian AR values fluctuate between 1.6 × 10^6 and 4.2 × 10^7 tests/cm/k.y.

An interesting feature is that all siliceous organisms show both very low absolute abundances and accumulation rates at the Stage 5/6 boundary, a time of very low diatom diversity. This may point to a dissolution level also observed by Jansen and van Iperen (1991) in the Congo Fan area.

F6. Continental signal based on relative contributions of continental organisms, p. 22.

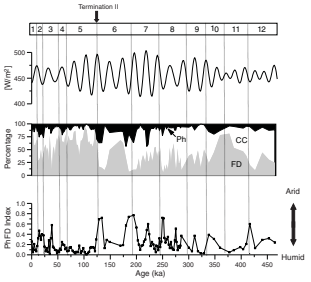

DISCUSSION: TEMPORAL FLUCTUATIONS IN THE COMPOSITION OF SILICEOUS MICROFOSSIL ASSEMBLAGES

Marine Signal

A total of 154 diatom taxa were identified and counted. The most common taxa (28, with an overall average contribution of >1%) are summarized in Table T3. Marine diatoms dominate the assemblage in terms of relative contribution (~97% marine vs. ~3% freshwater), as well as concentrations per gram, and accumulation rates (see "Sedimentation Rates," p. 6, and "Siliceous Organisms," p. 7, both in "Results").

In the sediments of the Congo Fan, van Iperen et al. (1987) defined six marine diatom groups in surface sediments that reflect properties of the overlying water masses. Essentially, we keep their groupings with

slight modifications based on our own experience with temporal and spatial distribution of diatom species in sediment traps and surface sediments in the equatorial and tropical Atlantic (summary in Romero et al., 1999a), including additional observations of Pokras and Molfino (1986). The composition of the resulting seven groups and their preferred environmental conditions is given in Table T3, their distribution downcore is illustrated in Figure F7, and their concentration per gram dry sediment is summarized in Table T4.

In accordance with the results of van Iperen et al. (1987), the marine diatom assemblage is dominated by two neritic, high-nutrient indicators, *T. nitzschioides* var. *nitzschioides* and resting spores of the genus *Chaetoceros,* and by *C. litoralis*. The latter can be considered a plume-related species in the Congo and the Niger area (van Iperen et al., 1987; Pokras, 1991). It is possible that in these previous studies, *C. litoralis* was misidentified as *C. striata* (van Iperen, pers. comm, 1999). Although little is known about the ecological preferences of *C. litoralis,* the species has been recurrently found in neritic environments with highly variable salinities (C. Lange, unpubl. data). Fluctuations in relative abundance and accumulation rates of this species at Site 1077 suggest two long-term periods of lowered salinity and enhanced river discharge, between 220 and 325 ka (moderate) and in the last 125 ka, including two strong pulses at 10–50 ka and 75–125 ka.

The occurrence of *Chaetoceros* spp. resting spores and remains of vegetative cells in the Congo area can be attributed to seasonal variability of coastal upwelling and nutrient input from the river outflow (the Congo effect) and probably also reflects advection from the shelf (see discussion in Jansen and van Iperen, 1991). They are common members of the diatom assemblage (~20%), and their abundance pattern shows high variability, especially during the past 250 k.y. Maxima in the relative abundance are seen during interglacial stages (Fig. F7).

We consider the record of *T. nitzschioides* var. *nitzschioides* as indicative of increased nutrient supply by the coastal upwelling process, in agreement with Jansen and van Iperen (1991), rather than of river influence (Pokras and Molfino, 1986). At Site 1077, a long-term trend is evident with a clear dominance (>50%) during 460–125 ka, dropping to low levels at Termination II (Fig. F7). On shorter time scales, abundance peaks are generally associated with glacial periods.

The presence of the littoral group (composed of benthic, tycopelagic, epiphytic species, etc.) is constant but rare (~1%); moderate peaks occurred during interglacials. A significant (5% confidence level) difference in average concentration between glacial and interglacial times was found (Student's t test; Sokal and Rohlf, 1973): TT = 4.669, theoretic t-value = 2.626. The warm-water group was always present in low numbers (highest peak in Stage 11) as an indication that our study area has always been under the influence of warm and saline waters of the SECC. Episodic maxima of the oceanic temperate assemblage may be associated with cold water intrusions of the BC.

It is interesting to note two time intervals with prominent peaks in the relative abundance of a cold water silicoflagellate, *Dictyocha speculum* (at ~25 and 40–50 ka), and of the oceanic temperate diatom assemblage (at 40–70 and 225 ka) (Fig. F8). In particular, the period 15–65 ka, and to a lesser extent 80–100 ka, coincides with high diatom accumulation rates and lower sea-surface temperatures (Schneider et al., 1995) in the Congo Fan area (Fig. F8). These observations correlate well with inferences made by Jansen et al. (1996) of northward movements of the ABF. Although the peaks may not represent BCC waters per se (Jansen et

F7. Accumulation rates and relative abundances of the marine diatom groups present at Site 1077, p. 23.

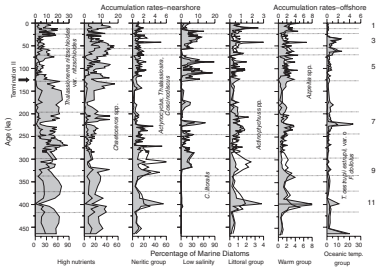

T4. Concentrations of marine diatom groups, Site 1077, p. 30.

F8. Diatom accumulation rates and contribution of cold-temperate water taxa compared to sea-surface temperature estimates from GeoB 1008, and the reconstruction of the position of the Angola-Benguela Front, p. 24.

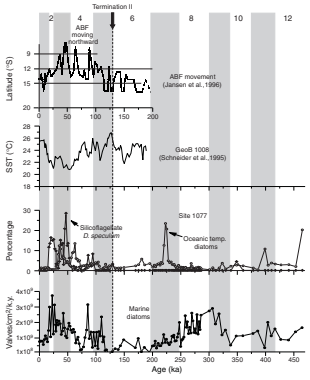

al., 1996), we suggest that these times are characterized by enhanced productivity caused by frontal mixing of cold, nutrient-rich waters from the south (Fig. F8) and river-induced upwelling from the coast (high abundances of *Chaetoceros* spp. and *C. litoralis*) (Fig. F7). We do not know if the 225-ka peak can also be related to an earlier northerly position of the ABF.

Continental Signal

The presence of freshwater diatoms and phytoliths in marine sediments from the Atlantic Ocean is attributed to three different transport mechanisms: eolian, fluvial, and transport by turbidity currents (Pokras, 1991; Pokras and Mix, 1985; van Iperen et al., 1987; Gasse et al., 1989; Stabell, 1986; Treppke, 1996). The interpretation of these siliceous remains in the water column and sediments raises the problem of identifying their source area and transporting agents. In the equatorial and tropical regions between 20°N and 10°S and west of 2°E, eolian transport with direct settling over the open ocean is assumed to be the main transport mechanism of freshwater diatoms and phytoliths (Pokras, 1991; Pokras and Mix, 1985; Stabell, 1986; Gasse et al., 1989; Romero et al., 1999b). In contrast, in nearshore areas influenced by river discharge (e.g., Niger, Congo, and Amazonas), fluvial transport is responsible for the deposition of freshwater diatoms, phytoliths, and other continental remains (Melia, 1984; Gasse et al., 1989; van Iperen et al., 1987; Jansen and van Iperen, 1991). Site 1077 is strongly influenced by Congo River discharge (Fig. F1); it lies outside of the turbidite fan area (van Weering and van Iperen, 1984; van Iperen et al., 1987; Pufahl et al., 1998). Although eolian influence at our study site cannot be completely ruled out as a possible mechanism of deposition of continental remains, wind contribution is probably minor when compared to the riverine input. The continental signal recorded by freshwater diatoms is dominated by the genus *Aulacoseira* (mostly *Aulacoseira granulata* and *Aulacoseira islandica*), which represents an average of 64% of the freshwater assemblage (Table T3). Other freshwater species in sediments of Site 1077 include *Cyclotella meneghiniana, Luticola mutica,* and *Stephanodiscus astrea*. Their abundances may be underrepresented, because *Aulacoseira*-rich sediments from Site 1077 may also be a consequence of differential dissolution during transport within the river waters and discharge into the ocean, where dissolution increases as a result of low dissolved silica contents and high ionic concentration (van Bennekom and Berger, 1984; Hurd, 1983). However, *Aulacoseira* species are commonly found in African water bodies, especially in the Congo River, where the genus makes up 80% of the total diatom population (Gasse et al., 1989). We believe that *Aulacoseira* values (and total freshwater loads) at Site 1077 are useful for reconstructing temporal fluctuations in the intensity of Congo River discharge. They reflect humid periods with increased rainfall and river discharge fostered by an intensified monsoon during times of maximum insolation in the Northern Hemisphere (Fig. F6) (Schneider et al., 1997; Gingele et al., 1998).

The continental signal derived from chrysophycean cysts is probably related to both humidity on land and changes in the Congo drainage area and inland water bodies. An interesting long-term contrasting trend is evident when comparing freshwater diatom and chrysophycean cyst records, with chrysophycean cysts being more abundant between 460 and 125 ka (except for two freshwater diatom maximas at ~170 and ~370 ka) and freshwater diatoms dominating during the last

122 k.y. (Fig. F6). Because chrysophycean cysts are of limnic origin, we speculate that their higher values prior to Termination II may be attributed to a larger number of lakes drained by the Congo. Apparently, pre-Pleistocene times were characterized by lakes and swamps covering a large area around the Congo River (Beadle, 1974). Changes in vegetation were also recorded. A drop in the proportion of plants of the family Cyperaceae at and around Termination II was reported by Dupont et al. (1999). This family includes aquatic plants adapted to life in marshy and freshwater environments.

Our third continental proxy, the contribution of phytoliths, does not show marked long-term changes. Phytoliths were almost always present in much lower numbers than freshwater diatoms and chrysophycean cysts; highest relative abundances were observed during Stages 6 and 7 (Fig. F6). On the other hand, the PhFD index shows a spiky pattern with a moderate long-term trend pointing to more arid conditions on land prior to ~122 ka and more humid conditions thereafter.

CONCLUSIONS

1. Sediments from Site 1077 contain large amounts of siliceous microfossils. The marine signal dominates, and marine diatoms are the most abundant siliceous microfossils group, followed by silicoflagellates and radiolarians.
2. High abundances of diatoms, silicoflagellates, and radiolarians point to increased productivity during glacial stages and cooler conditions of Substages 5.2 and 5.4.
3. An abrupt change in the amplitude of the siliceous signal as well as in the diatom assemblages is evident at Termination II. The system seems to change from predominantly marine to marine/brackish.
4. The continental signal derived from freshwater diatoms shows two periods that can be correlated with humid conditions on land and/or northward movements of the Congo River plume during Stages 10 and 11 and during 28–119 ka.
5. Fluctuations in the abundances of chrysophycean cysts may be used as indicators of changes in the extension of inland waters. They point to an abrupt reduction of the limnetic system, particularly during the last 125 k.y.
6. Sedimentation rates showed highest values at Stage 11, between Stages 9 and 7, and between Stages 5 and 1 in correspondence to the northward movements of the ABF detected by the oceanic temperate diatom assemblage in combination with *D. speculum* (cold-water silicoflagellate).
7. The opal signal recorded at Site 1075 correlates well with concentration of marine diatoms at the Site 1077 from ~120 ka to the present; differences in timing can be attributed to differences on the age model. Both parameters showed higher values during the last 125 k.y.
8. TOC in sediments from Site 1075 is of marine origin, in agreement with the overwhelming dominance of marine siliceous microfossils.

ACKNOWLEDGMENTS

This study was supported by the Deutsche Forschungsgemeinschaft (Sonderforschungs-bereich 261 at the Bremen University). We thank the ODP technicians and the drilling crew for their efforts in sediment recovery. We acknowledge fruitful discussions with Lydie Dupont, Britta Jahn, Fred Jansen, and Jolanda van Iperen during Leg 175 and postcruise. We would like to thank U. Zielinski, J. Whitehead, and an anonymous reviewer for their suggestions, which helped improve the final version.

REFERENCES

Alexander, A., Meunier, J.D., Lézime, A.M., Vicens, A., and Schwartz, D., 1997. Phytolits: indicators of grassland dynamics during the late Holocene in intertropical Africa. *Palaeoceanogr., Palaeoclimatol., Palaeoecol.,* 136:213–229.

Beadle, L.C., 1974. *The Inland Waters of Tropical Africa: an Introduction to Tropical Limnology:* London (Longman).

Berger, A., and Loutre, M.F., 1991. Insolation values for the climate of the last 10 million years. *Quat. Sci. Rev.,* 10:297–317.

Berger, W.H., Smetacek, V.S., and Wefer, G., 1989. Ocean productivity and paleoproductivity: an overview. *In* Berger, W.H., Smetacek, V.S., and Wefer, G. (Eds.), *Productivity of the Oceans: Present and Past:* New York (Wiley & Sons), 1–34.

Cadée, G.C., 1978. Primary production and chlorophyll in the Zaire river, estuary and plume. *Neth. J. Sea Res.,* 12:368–381.

————, 1984. Particulate and dissolved organic carbon and chlorophyll a in the Zaire river, estuary and plume. *Neth. J. Sea Res.*, 17:426–440.

Dupont, L., Schneider, R., Schmüser, A., and Jahns, S., 1999. Marine-terrestrial interaction of climate changes in West Equatorial Africa of the last 190,000 years. *Paleoceanogr. Afr.,* 26:61–84.

Dupont, L.M., Donner, B., Schneider, R., and Wefer R., in press. Mid-Pleistocene environmental change in tropical Africa began as early as 1.05 Ma. *Geology.*

Dupont, L.M., Jahns, S., Marret, F., and Ning, S., 2000. Vegetation change in equatorial West Africa: time-slices for the last 150 ka. *Palaeoceanogr., Palaeoclimatol., Palaeoecol.,* 155:95–122.

Eisma, D., and van Bennekom, A.J., 1978. The Zaire River and estuary and the Zaire outflow in the Atlantic Ocean. *Neth. J. Sea Res.,* 12:255–272.

Gasse, F., Stabell, B., Fourtanier, E., and van Iperen, Y., 1989. Freshwater diatom influx in intertropical Atlantic: relationships with continental records from Africa. *Quat. Res.,* 32:229–243.

Gingele, F.X., Müller, P.M., and Schneider, R.R., 1998. Orbital forcing of freshwater input in the Zaire Fan area: clay mineral evidence from the last 200 kyr. *Palaeoceanogr., Palaeoclimatol., Palaeoecol.,* 138:17–26.

Hurd, D.C., 1983. Physical and chemical properties of siliceous skeletons. *In* Aston, S.R. (Ed.), *Silicon Geochemistry and Biogeochemistry:* London (Academic Press), 187–244.

Jansen, J.H.F., 1984. Structural and sedimentary geology of the Congo and southern Gabon continental shelf: a seismic and acoustic reflection survey. *Neth. J. Sea Res.,* 17:164–384.

————, 1985. Middle and Late Quaternary carbonate production and dissolution, and paleoceanography of the eastern Angola Basin, South Atlantic Ocean. *In* Hsü, K.J., and Weissert, H.J. (Eds.), *South Atlantic Paleoceanography:* Cambridge (Cambridge Univ. Press), 25–46.

Jansen, J.H.F., Alderliesten, C., Houston, C.M., de Jong, A.F.M., van der Borg, K., and van Iperen, J.M., 1989. Aridity in equatorial Africa during the last 225,000 years: a record of opal phytoliths/freshwater diatoms from the Zaire (Congo) deep-sea fan (northeast Angola basin). *Radiocarbon,* 31:557–569.

Jansen, J.H.F., Ufkes, E., and Schneider, R.R., 1996. Late Quaternary movements of the Angola-Benguela-Front, SE Atlantic, and implications for advection in the equatorial ocean. *In* Wefer, G., Berger, W.H., Siedler, G., and Webb, D. (Eds.), *The South Atlantic: Present and Past Circulation:* Berlin (Springer-Verlag), 553–575.

Jansen, J.H.F., and van Iperen, J.M., 1991. A 220,000-year climatic record for the east equatorial Atlantic Ocean and equatorial Africa: evidence from diatoms and opal phytoliths in the Zaire (Congo) deep-sea fan. *Paleoceanography,* 6:573–591.

Jansen, J.H.F., van Weering, T.C.E., Gieles, R., and van Iperen, J., 1984. Middle and late Quaternary oceanography and climatology of the Zaire-Congo fan and the adjacent eastern Angola Basin. *Neth. J. Sea Res.,* 17:201–249.

Lange, C.B, Berger, W.H., Lin, H.-L., Wefer, G., and Shipboard Scientific Party, 1999. The early Matuyama diatom maximum off SW Africa, Benguela Current System (ODP Leg 175). *Mar. Geol.,* 161:93–114.

Lange, C.B., Treppke, U.F., and Fischer, G., 1994. Seasonal diatom fluxes in the Guinea Basin and their relationship to trade winds, hydrography and upwelling events. *Deep-Sea Res.,* 41:859–878.

Lin, H.-L., Lin, C.Y., Meyers, P., and Adams, D., in press. Biogenic opal and organic carbon isotope evidence of late Quaternary variations in marine productivity along the southwest African margin. *Mar. Geol.*

Melia, M.B., 1984. The distribution and relationship between palynomorphs in aerosols and deep-sea sediments off the coast of Northwest Africa. *Mar. Geol.,* 58:345–371.

Mikkelsen, N., 1984. Diatoms in the Zaire deep-sea fan and Pleistocene palaeoclimatic trends in the Angola Basin and west equatorial Africa. *Neth. J. Sea Res.,* 17:280–292.

Mortlock, R.A., and Froelich, P.N., 1989. A simple method for the rapid determination of biogenic opal in pelagic marine sediments. *Deep-Sea Res. Part A,* 36:1415–1426.

Müller, P.J., and Schneider, R., 1993. An automated leaching method for the determination of opal in sediments and particulate matter. *Deep-Sea Res.,* 40:425–444.

Pastouret, L., Chamley, H., Delibrias, G., Duplessy, J.-C., and Thiede, J., 1978. Late Quaternary climatic changes in western tropical Africa deduced from deep-sea sedimentation off the Niger delta. O*ceanol. Acta,* 1:217–232.

Pokras, E.M., 1991. Source areas and transport mechanisms for freshwater and brackish-water diatoms deposited in pelagic sediments of the Equatorial Atlantic. *Quat. Res.,* 35:144–156.

Pokras, E.M., and Mix, A.C., 1985. Eolian evidence for spacial variability of late Quaternary climates in tropical Africa. *Quat. Res.,* 24:137–149.

Pokras, E.M., and Molfino, B., 1986. Oceanographic control of diatom abundances and species distributions in surface sediments of the tropical and southeast Atlantic. *Mar. Micropaleontol.,* 10:165–188.

Pufahl, P.K., Maslin, M.A., Anderson, L., Brüchert, V., Jansen, F., Lin, H., Perez, M., Vidal, L., and Shipboard Scientific Party, 1998. Lithostratigraphic summary for Leg 175: Angola–Benguela upwelling system. *In* Wefer, G., Berger, W.H., and Richter, C., et al., *Proc. ODP, Init. Repts.,* 175: College Station, TX (Ocean Drilling Program), 533–542.

Romero, O.E., Lange, C.B., Fischer, G., Treppke, U.F., and Wefer, G., 1999a. Variability in export production documented by downward fluxes and species composition of marine planktonic diatoms: observations from the tropical and equatorial Atlantic. *In* Fischer, G., and Wefer, G. (Eds.), *Use of Proxies in Paleoceanography: Examples from the South Atlantic:* Berlin (Springer-Verlag), 365–392.

Romero, O.E., Lange, C.B., Swap, R.J., and Wefer, G., 1999b. Eolian transported freshwater diatoms and phytoliths across the equatorial Atlantic record of temporal changes in Saharan dust transport patterns. *J. Geophys. Res.,* 104:3211–3222.

Runge, F., 1999. The opal phytolith inventory of soils in central Africa: quantites, shapes, classification, and spectra. *Rev. Paleobot. Palynol.,* 107:23–53.

Schneider, R., 1991. Spätquartäre Produktivitätsänderungen im östlichen Angola-Becken: Reaktion auf Variationen im Passat-Monsun-Windsystem und in der Advektion des Benguela-Küstenstroms [Ph.D. thesis]. *Ber. Fachber. Geowiss.,* 21. Univ. Bremen, Germany.

Schneider, R., Müller, P.J., and Wefer, G., 1994. Late Quaternary productivity changes off the Congo deduced from stable carbon isotopes of planktonic foraminifera. *Palaeogeogr., Palaeoclimatol., Palaeoecol.,* 110:255–274.

Schneider, R.R., Müller, P.J., and Ruhland, G., 1995. Late Quaternary surface circulation in the east equatorial South Atlantic: evidence from alkenone sea surface temperatures. *Paleoceanography,* 10:197–219.

Schneider, R.R., Müller, P.J., Ruhland, G., Meinecke, G., Schmidt, H., and Wefer, G., 1996. Quaternary surface temperatures and productivity in the Equatorial South Atlantic: response to changes in Trade Monsoon wind forcing and surface water advection. *In* Wefer, G., Berger, W.H., Siedler, G., and Webb, D.J. (Eds.), *The South Atlantic: Present and Past Circulation:* Berlin (Springer-Verlag), 527–551.

Schneider, R.R., Price, B., Müller, P.J., Kroon, D., and Alexander, I., 1997. Monsoon-related variations in Zaire (Congo) sediment load and influence of fluvial silicate supply on marine productivity in the east equatorial Atlantic during the last 200,000 years. *Paleoceanography,* 12:463–481.

Schrader, H.J., and Gersonde, R., 1978. Diatoms and silicoflagellates. *In* Zachariasse, W.J., et al. (Eds.), *Micropaleontological Counting Methods and Techniques: An Exercise of an Eight Metres Section of the Lower Pliocene of Cap Rossello, Sicily.* Utrecht Micropaleontol. Bull., 17:129–176.

Shackleton, N.J., Berger, A., and Peltier, W.A., 1990. An alternative astronomical calibration of the lower Pleistocene timescale based on ODP Site 677. *Trans. R. Soc. Edinburgh: Earth Sci.,* 81:251–261.

Shackleton, N.J., and Opdyke, N.D., 1973. Oxygen isotope and paleomagnetic stratigraphy of equatorial Pacific core V28-238: oxygen isotope temperatures and ice volumes on a 10^5 year and 10^6 year scale. *Quat. Res.,* 3:39–55.

Shipboard Scientific Party, 1998a. Introduction: background, scientific objectives, and principal results for Leg 175 (Benguela Current and Angola-Benguela upwelling systems). *In* Wefer, G., Berger, W.H., and Richter, C., et al., *Proc. ODP, Init. Repts,* 175: College Station, TX (Ocean Drilling Program), 7–25.

————, 1998b. Site 1075. *In* Wefer, G., Berger, W.H., and Richter, C., et al., *Proc. ODP, Init. Repts.,* 175: College Station, TX (Ocean Drilling Program), 49–86.

————, 1998c. Site 1077. *In* Wefer, G., Berger, W.H., and Richter, C., et al., *Proc. ODP, Init. Repts.,* 175: College Station, TX (Ocean Drilling Program), 115–141.

Showers, W.J., and Bevis, M., 1988. Amazon Cone isotopic stratigraphy: evidence for the source of the tropical freshwater spike. *Palaeogeogr., Palaeoclimatol., Palaeoecol.,* 64:189–199.

Smol, J.P., 1988. Chrysophycean microfossils in paleolimnological studies. *Palaeogeogr., Palaeoclimatol., Palaeoecol.,* 62:287–297.

Sokal, R.R., and Rohlf, F.J., 1973. Single classification analysis of variance. *In* Kennedy, D., and Park, R.B. (Eds.), *Introduction to Biostatistics:* San Francisco (W.H. Freeman), 161–179.

Stabell, B., 1986. Variations of diatom flux in the eastern equatorial Atlantic during the last 400,000 years ("Meteor" cores 13519 and 13521). *Mar. Geol.,* 72:305–323.

Treppke, U., 1996. Saisonalität im Diatomeen- und Silikoflagellatenfluβ im Östlichen tropischen und subtropichen Atlantik [Ph.D. thesis]. *Ber. Fachber. Geowiss.,* 74. Univ. Bremen, Germany.

van Andel, T.H., Heath, G.R., and Moore, T.C., Jr., 1975. Cenozoic history and paleoceanography of the central equatorial Pacific Ocean: a regional synthesis of Deep Sea Drilling Project data. *Mem.—Geol. Soc. Am.,* 143.

van Bennekom, A.J., and Berger, G.W., 1984. Hydrography and silica budget of the Angola Basin. *Neth. J. Sea Res.,* 17:149–200.

van der Gaast, S.J., and Jansen, J.H.F., 1984. Mineralogy, opal, and manganese of Middle and Late Quaternary sediments of the Zaire (Congo) deep-sea fan: origin and climatic variation. *Neth. J. Sea Res.,* 17:313–341.

van Iperen, J.M., van Weering, T.C.E., Jansen, J.H.F., and van Bennekom, A.J., 1987. Diatoms in surface sediments of the Zaire deep-sea fan (SE Atlantic Ocean) and their relation to overlying water masses. *Neth. J. Sea Res.,* 21:203–217.

van Weering, T.C.E., and van Iperen, J., 1984. Fine-grained sediments of the Zaire deep-sea fan, southern Atlantic Ocean. *In* Stow, D.A.V., and Piper, D.J.W. (Eds.), *Fine-Grained Sediments: Deep Water Processes and Facies:* Oxford (Blackwell), 95–113.

Figure F1. Location of Sites 1077, 1075, and GeoB1008 and main surface and subsurface currents and areas with high primary productivity in the eastern Angola Basin. Modified from Schneider et al. (1994).

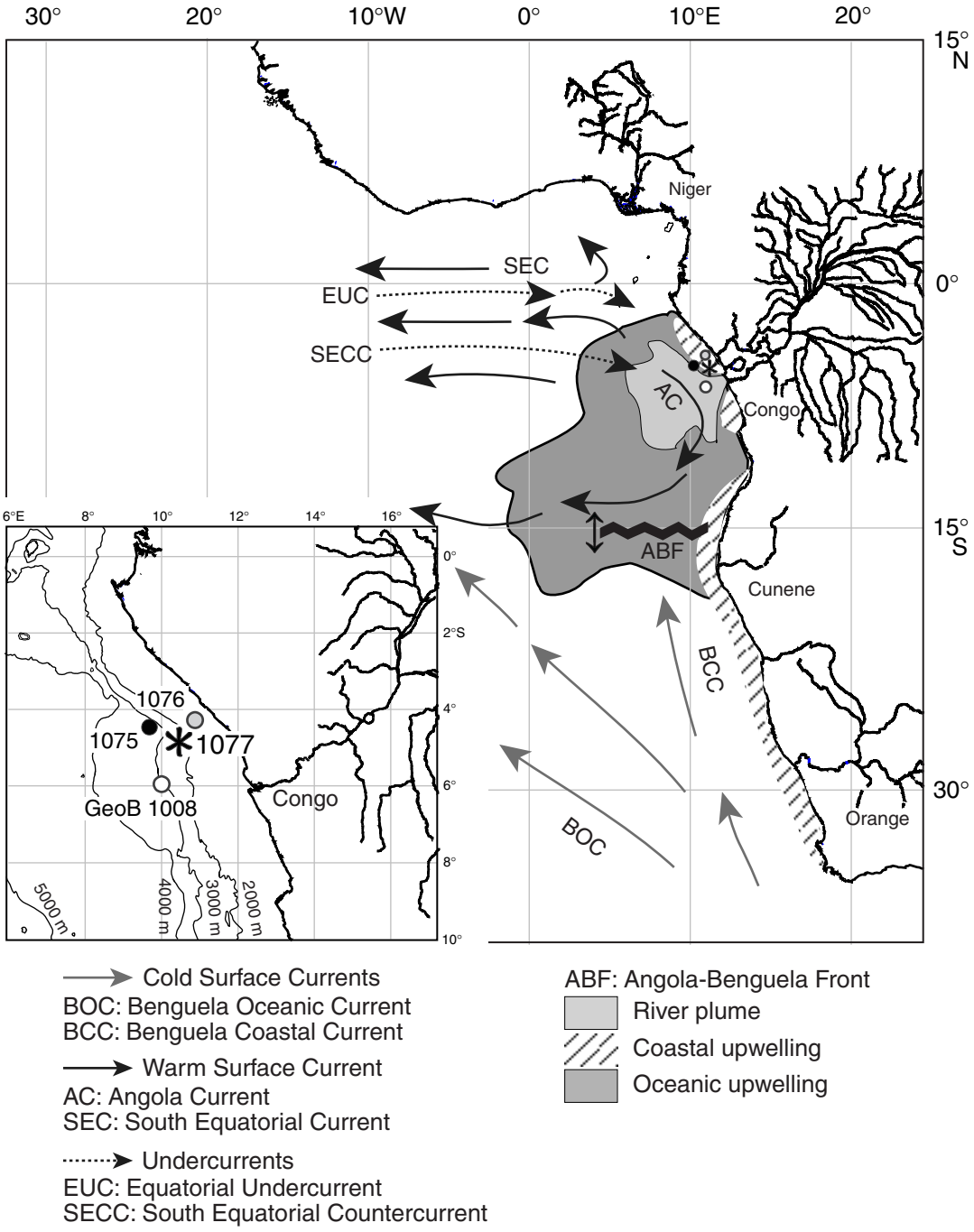

Figure F2. Comparison of Sites 1077 (this work) and 1075 (Lin et al., in press) with core GeoB1008 (Schneider, 1991): $\delta^{18}O$, sedimentation rates, organic carbon, and opal records. Head bars and shaded/white columns denote SPECMAP oxygen isotope stages. MOC = marine organic carbon, TOC = total organic carbon.

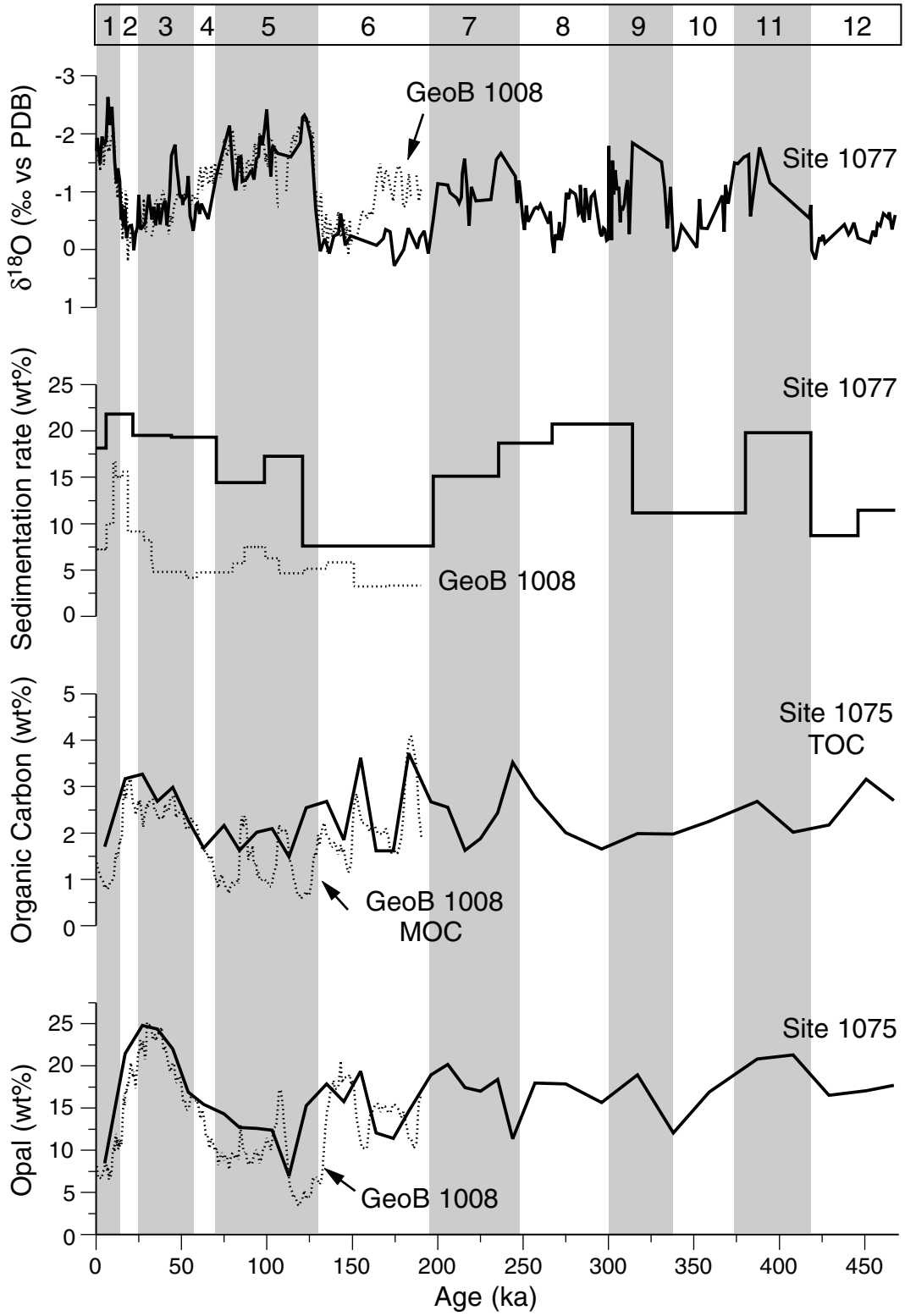

Figure F3. Age model used at Site 1077 based on $\delta^{18}O$ data of the planktonic foraminifer *Globigerinoides ruber* pink.

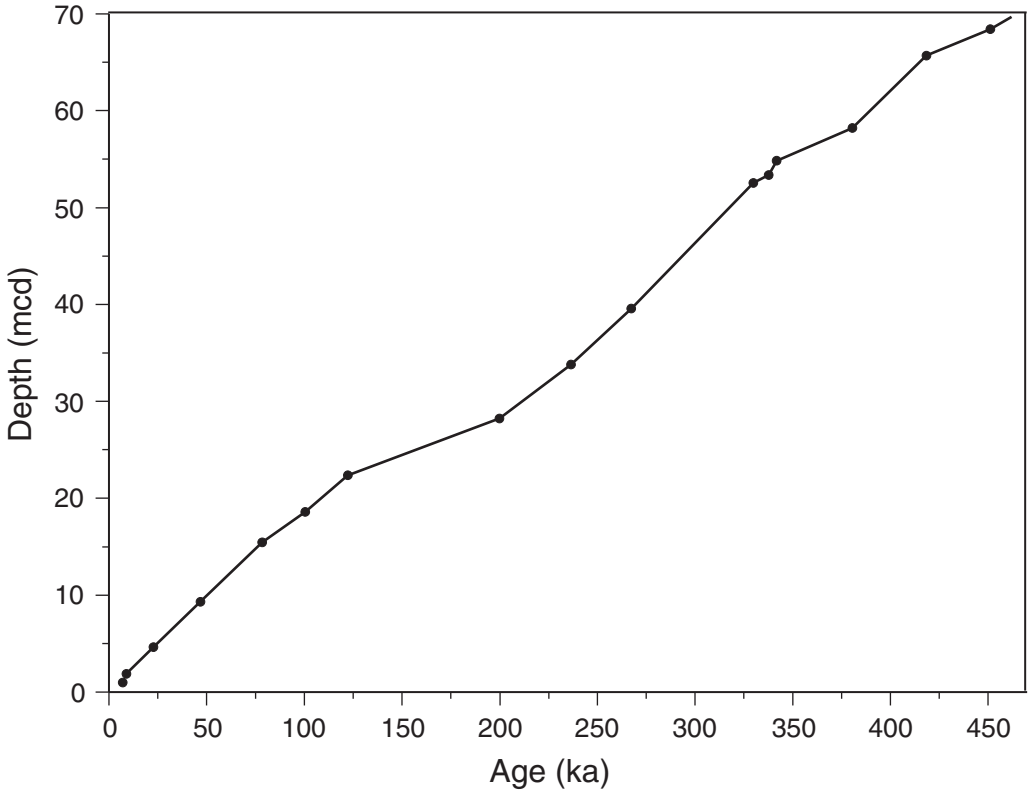

Figure F4. Abundances of the most abundant siliceous microfossils counted. Horizontal lines refer to the average value of each group and are for guidance. Head bars and shaded/white columns denote SPECMAP oxygen isotope stages.

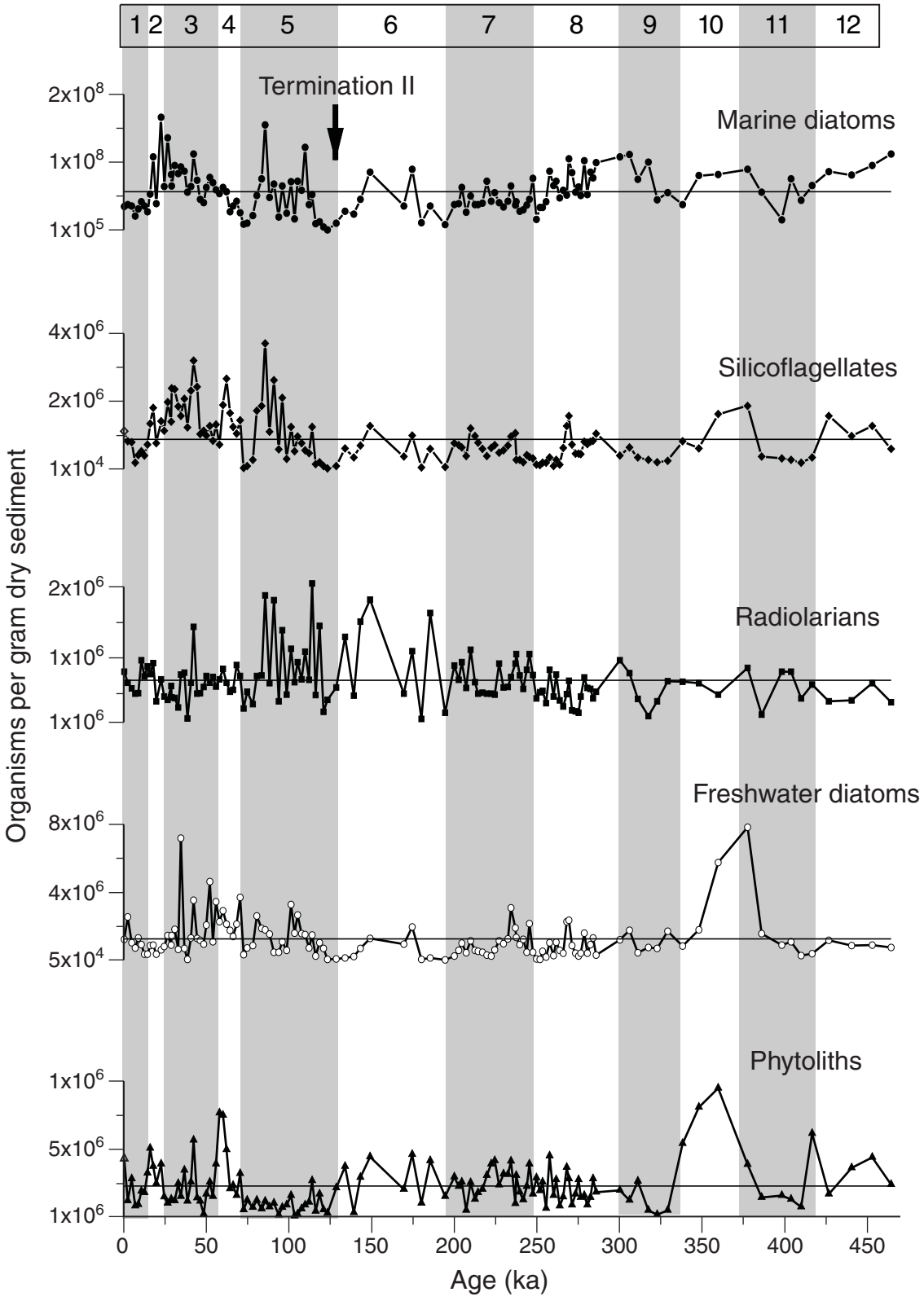

Figure F5. Marine signal. Accumulation rates of marine diatoms, silicoflagellates, and radiolarians, sedimentation rates, the $\delta^{18}O$ record for Site 1077, and opal for GeoB1008. Head bars and shaded/white columns denote SPECMAP oxygen isotope stages.

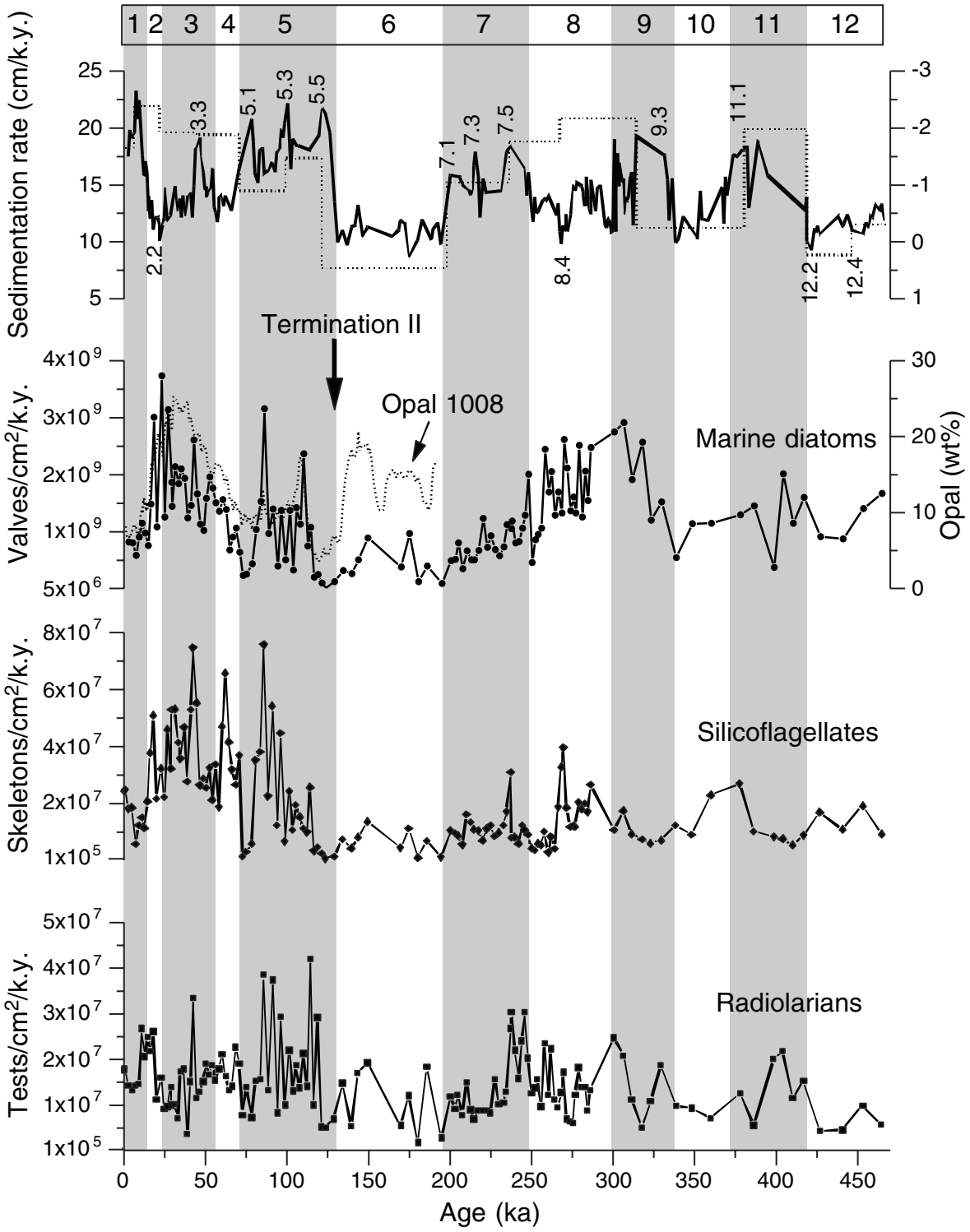

Figure F6. Continental signal. Relative contributions of freshwater diatoms (FD), chrysophycean cysts (CC), and phytoliths (Ph) based on the assumption that 100% continental signal is equal to the sum of individual percentages. PhFD index of Jansen and van Iperen (1991) vs. precessional oscillation of boreal summer insolation (July) at 15°N (data from Berger and Loutre, 1991). Head bars and columns denote SPECMAP oxygen isotope stages.

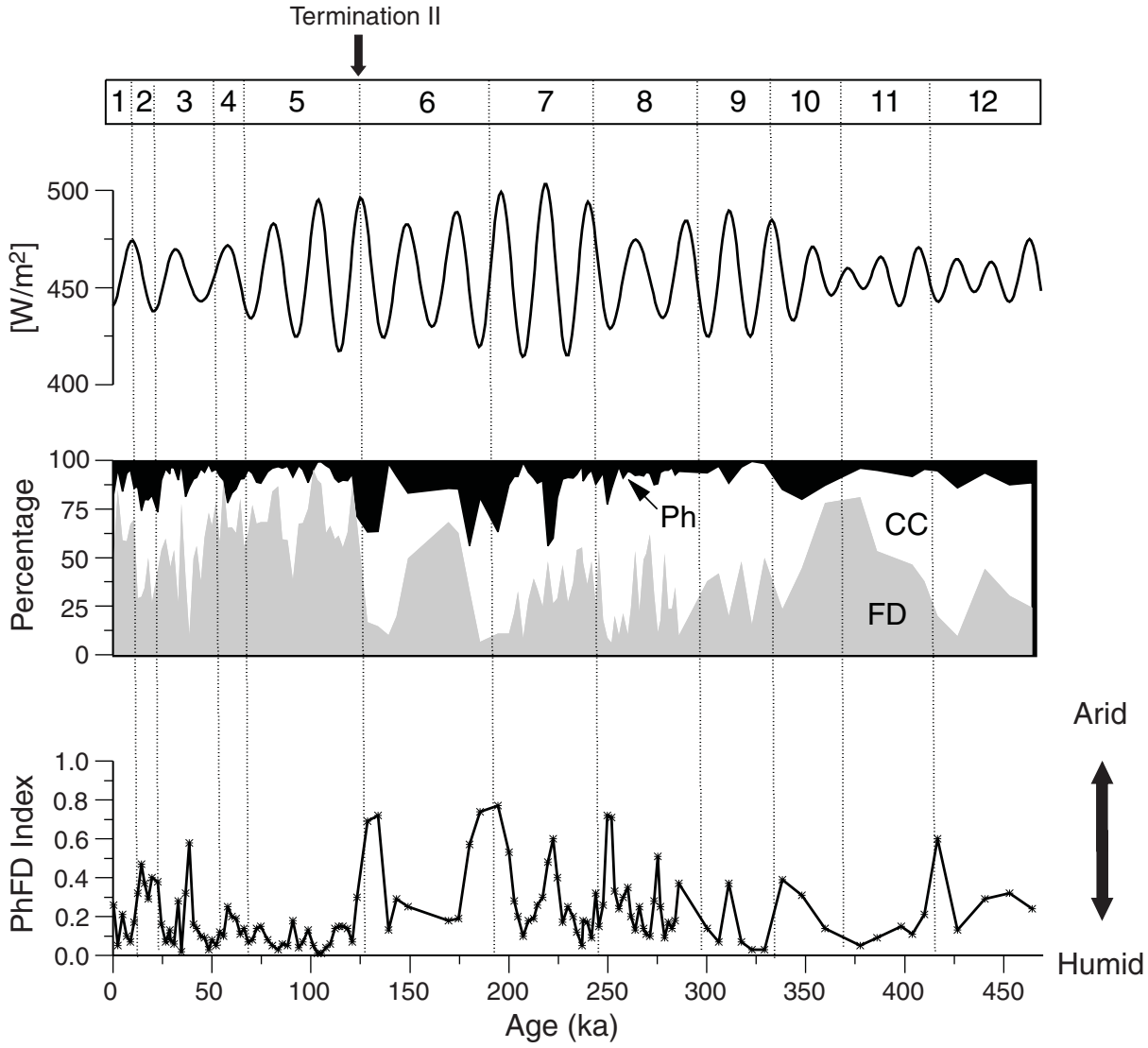

Figure F7. Accumulation rates (solid line upper axes) and relative abundances (shaded area, lower axes) of the marine diatom groups present at Site 1077. Diatom groupings follow van Iperen et al. (1987) and Romero et al. (1999a). The scale for accumulation rates is valves × 10^7/cm²/k.y. for the littoral and the warm groups; all other scales are valves × 10^8/cm²/k.y.

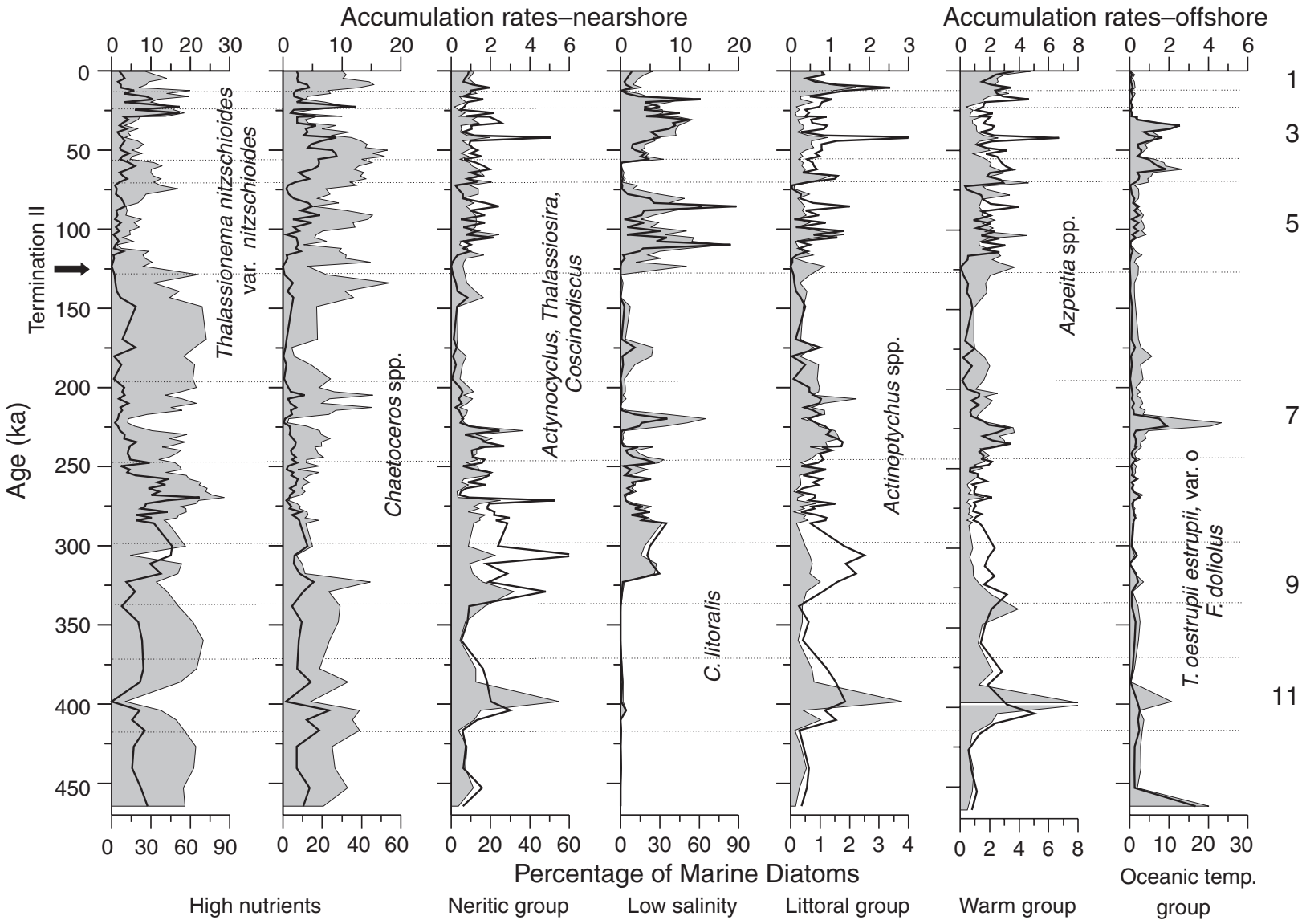

Figure F8. Marine diatom accumulation rates and relative contribution of cold-temperate water taxa compared to sea-surface temperature (SST) estimates from a nearby core, GeoB 1008 (from Schneider et al., 1995), and the reconstruction of the average position of the Angola-Benguela Front (modified from Jansen et al., 1996). Head bars and shaded/white columns denote SPECMAP oxygen isotope stages.

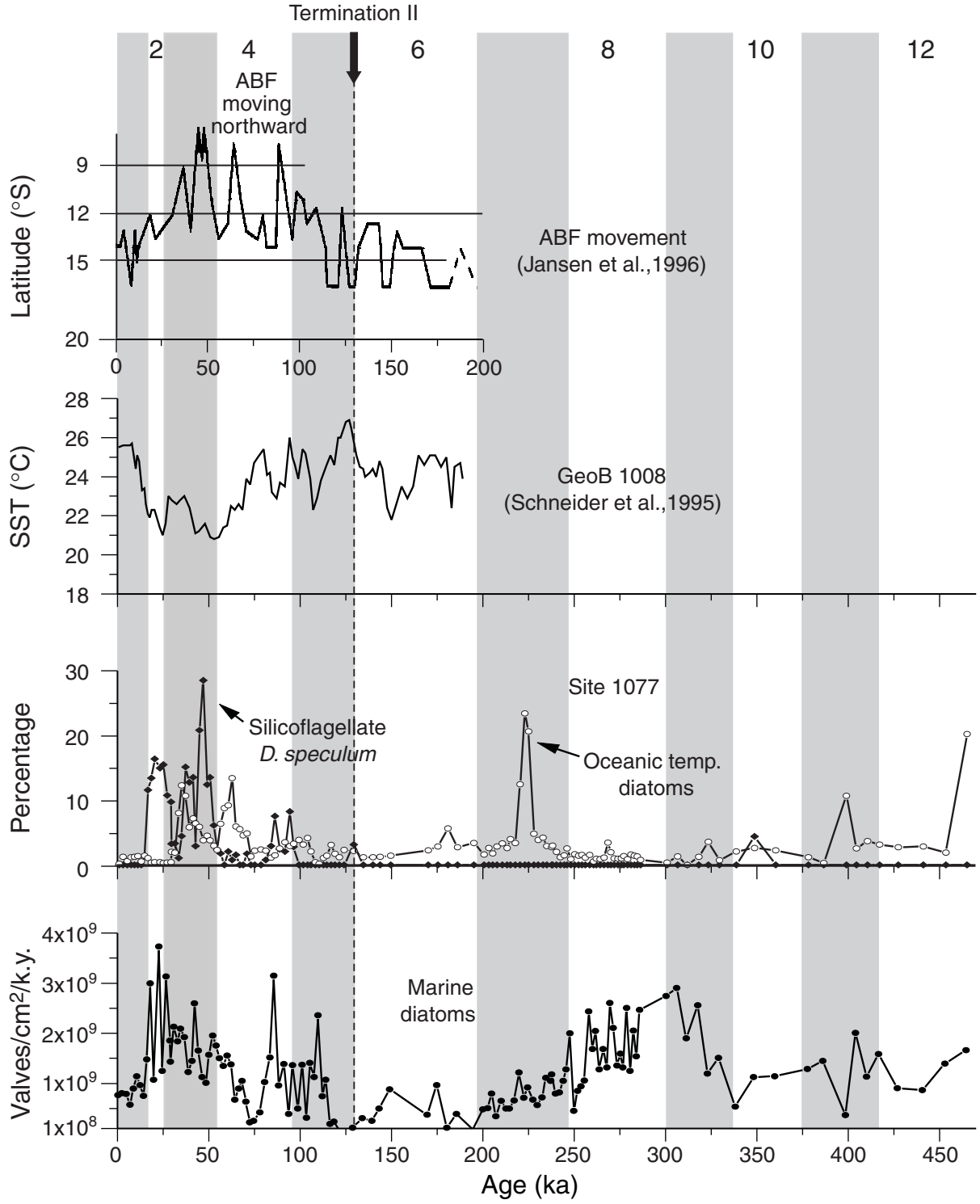

Table T1. Age model used at Site 1077.

Core, section, interval (cm)	Depth (mcd)	Age (ka)
175-1077B-		
1H-1, 85-88	0.85	6
1H-2, 25-28	1.75	8
1H-4, 5-8	4.55	22
2H-3, 65-68	9.25	46
175-1077A-		
3H-1, 48-50	15.42	78
3H-3, 65-68	18.59	100
3H-5, 145-148	22.39	122
4H-3, 85-88	28.29	200
4H-7, 45-48	33.89	237
5H-4, 125-128	39.69	268
6H-5, 45-48	52.77	331
6H-5, 125-128	53.57	339
6H-6, 125-128	55.07	343
7H-2, 25-28	58.45	382
7H-7, 24-26	65.98	420
8H-2, 105-107	68.75	453
8H-4, 125-128	71.95	481
9H-4, 25-28	81.63	550
10H-4, 65-68	92.13	617
10H-5, 65-68	93.43	626
11H-5, 45-48	103.13	690
11H-6, 25-28	104.43	722
12H-1, 43-45	107.15	750
12H-2, 25-28	108.47	771
12H-4, 85-88	112.07	784
12H-5, 45-48	113.17	798
13H-1, 125-128	117.47	846
13H-2, 125-128	118.77	857
13H-3, 45-48	119.67	872

Note: Age model is based on the $\delta^{18}O$ record of *Globigerinoides ruber* (pink), based on tie points that were aligned with the record from Site 677 (Panama Basin; Schackleton et al., 1990).

Table T2. Depth, density, sedimentation rate, and concentration of siliceous organisms, Site 1077. (Continued on next two pages).

Core, section, interval (cm)	Depth (mbsf)	Depth (mcd)	Age (ka)	Density (g/cm3)	Sedimentation rate (cm/k.y.)	Marine diatoms (organisms/g dry sediment)	Silicoflagellates (organisms/g dry sediment)	Radiolarians (organisms/g dry sediment)	Freshwater diatoms (organisms/g dry sediment)	Chrysophyceans cysts (organisms/g dry sediment)	Phytoliths (organisms/g dry sediment)
175-1077B-											
1H-1, 5-8	0.05	0.05	0.3	1.22	17.86	34,903,365	1,116,037	808,165	1,260,352	780,011	548,398
1H-1, 45-48	0.45	0.45	2.5	1.20	17.86	37,661,737	827,546	652,006	2,557,870	335,126	150,463
1H-1, 85-88	0.85	0.85	4.8	1.27	17.86	35,051,701	798,477	573,905	1,048,001	444,612	399,238
1H-1, 125-128	1.25	1.25	7.0	1.27	22.00	20,588,570	190,972	503,472	746,528	446,835	104,167
1H-2, 5-8	1.65	1.65	8.8	1.29	22.00	31,448,727	417,711	504,734	1,348,858	559,944	139,237
1H-2, 45-48	2.05	2.05	10.6	1.25	22.00	41,625,785	531,080	969,798	958,253	222,860	253,995
1H-2, 85-88	2.45	2.45	12.5	1.24	22.00	35,428,195	406,108	744,531	396,439	783,921	183,715
1H-2, 125-128	2.85	2.85	14.3	1.26	22.00	26,930,703	731,197	885,133	375,219	557,151	327,114
1H-3, 5-8	3.25	3.25	16.1	1.26	22.00	53,147,979	1,339,913	777,765	877,874	1,159,452	508,243
1H-3, 45-48	3.65	3.65	17.9	1.26	22.00	107,908,693	1,813,847	927,078	927,078	555,765	376,205
1H-3, 85-88	4.05	4.05	19.7	1.25	22.00	39,034,355	771,605	395,448	376,157	781,962	250,772
1H-3, 125-128	4.65	4.65	22.6	1.24	18.08	165,933,057	1,420,367	700,587	643,004	444,612	393,480
1H-4, 5-8	5.05	5.05	24.8	1.07	18.08	64,529,574	1,128,472	462,963	829,475	558,544	154,321
1H-4, 45-48	5.45	5.45	27.0	1.27	18.08	136,197,372	1,981,928	413,703	1,481,635	891,442	105,831
1H-4, 85-88	5.85	5.85	29.2	1.26	18.08	81,677,466	1,398,534	607,639	906,636	893,670	135,031
175-1077A-											
2H-1, 45-46	5.45	5.89	29.4	1.22	18.08	65,087,979	2,378,632	444,785	1,489,062	1,679,831	154,708
2H-1, 85-86	5.85	6.29	31.6	1.24	18.08	95,218,935	2,353,395	443,673	1,832,562	1,452,214	135,031
2H-1, 125-126	6.25	6.69	33.8	1.23	18.08	82,951,049	1,851,852	308,642	655,864	1,563,923	250,772
2H-2, 5-6	6.55	6.99	35.5	1.24	18.08	92,950,172	1,566,416	765,803	7,188,109	1,903,809	156,642
2H-2, 45-46	6.95	7.39	37.7	1.23	18.08	86,821,280	2,083,333	798,611	729,167	781,962	416,667
2H-2, 85-86	7.35	7.79	39.9	1.23	18.08	55,413,251	1,232,639	156,250	86,806	670,253	138,889
2H-2, 125-126	7.75	8.19	42.1	1.25	18.08	64,109,208	2,320,587	658,077	1,350,790	1,114,302	346,356
2H-3,5-6	8.05	8.49	43.8	1.28	18.08	112,165,708	3,202,451	1,438,782	3,562,146	2,239,775	742,597
2H-3, 45-46	8.45	8.89	46.0	1.24	18.24	73,214,405	2,424,494	502,217	1,316,154	2,005,744	173,178
2H-3, 85-86	8.85	9.29	48.2	1.25	19.90	45,157,221	1,044,277	504,734	1,209,621	671,933	156,642
2H-3, 125-126	9.25	9.69	50.2	1.26	19.90	40,325,869	1,131,300	591,757	983,361	335,966	34,809
2H-4, 5-6	9.55	9.99	51.7	1.27	19.90	62,469,528	1,000,585	750,439	2,097,380	891,442	192,420
2H-4, 45-46	9.95	10.39	53.7	1.26	19.90	77,739,039	1,273,148	655,864	4,639,275	1,005,379	327,932
2H-4, 85-86	10.35	10.79	55.7	1.26	19.90	70,135,953	831,554	734,862	1,121,631	671,933	212,723
175-1077B-											
2H-4, 104-105	11.14	11.14	57.5	1.27	19.90	59,202,575	1,319,444	601,852	3,472,222	0	462,963
2H-4, 144-145	11.54	11.54	59.5	1.26	19.90	53,742,031	727,238	702,160	2,282,022	446,835	927,855
2H-5, 35-36	11.95	11.95	61.6	1.24	19.90	62,927,788	1,885,718	846,649	2,924,787	780,011	865,891
2H-5, 75-76	12.35	12.35	63.6	1.23	19.90	56,518,145	2,666,944	656,153	2,137,788	780,011	613,820
2H-5, 115-116	12.75	12.75	65.6	1.25	19.90	26,921,723	1,655,093	526,620	1,780,478	223,418	225,694
2H-6, 4-5	13.14	13.14	67.5	1.27	19.90	35,503,891	1,253,858	551,698	1,429,398	893,670	275,849
2H-6, 44-45	13.54	13.54	69.6	1.25	19.90	42,334,113	1,053,241	902,778	2,156,636	1,117,088	200,617
2H-6, 84-85	13.94	13.94	71.6	1.26	19.90	25,294,548	1,450,848	750,439	3,727,179	780,011	425,249
175-1077C-											
3H-1, 105-106	14.35	14.35	73.6	1.30	19.90	8,727,198	42,545	293,945	351,960	111,989	69,618
3H-1, 145-146	14.75	14.75	75.6	1.29	19.90	9,740,010	100,560	529,874	760,002	223,978	162,443
175-1077A-											
3H-1, 48-50	14.98	15.42	79.0	1.24	15.85	21,492,044	279,707	356,867	887,346	335,126	77,160
3H-1, 85-88	15.35	15.79	81.3	1.27	15.85	51,128,420	1,729,681	752,315	2,617,027	372,363	128,601

Table T2 (continued).

Core, section, interval (cm)	Depth (mbsf)	Depth (mcd)	Age (ka)	Density (g/cm3)	Sedimentation rate (cm/k.y.)	Marine diatoms (organisms/g dry sediment)	Silicoflagellates (organisms/g dry sediment)	Radiolarians (organisms/g dry sediment)	Freshwater diatoms (organisms/g dry sediment)	Chrysophyceans cysts (organisms/g dry sediment)	Phytoliths (organisms/g dry sediment)
3H-1, 128-130	15.78	16.22	84.0	1.28	15.85	75,154,084	1,863,426	756,173	1,903,935	223,418	67,515
3H-2, 5	16.05	16.49	85.8	1.28	15.85	154,750,272	3,703,704	1,882,716	1,820,988	1,117,088	123,457
3H-2, 45-48	16.45	16.89	88.3	1.27	15.85	47,854,884	1,104,492	646,532	1,562,452	1,002,872	80,816
3H-2, 85-88	16.85	17.29	90.8	1.30	15.85	67,560,305	2,619,599	1,809,414	486,111	670,253	108,025
3H-2, 125-128	17.25	17.69	93.3	1.27	15.85	19,302,773	588,349	395,448	501,543	223,418	19,290
3H-3, 5-8	17.55	17.99	95.2	1.33	15.85	64,900,355	2,102,623	1,388,889	1,099,537	446,835	77,160
3H-3, 45-48	17.95	18.39	97.7	1.29	15.52	24,875,813	309,796	484,899	619,593	111,430	94,286
3H-3, 85-88	18.35	18.79	100.3	1.26	15.20	71,346,166	1,242,284	1,134,259	3,294,753	0	162,037
3H-3, 125-128	18.75	19.19	102.9	1.28	15.20	16,306,953	526,620	661,651	1,620,370	167,563	13,503
3H-4, 5-8	19.05	19.49	104.9	1.29	15.20	72,007,786	972,222	945,216	2,673,611	335,126	27,006
3H-4, 48-48?	19.48	19.92	107.8	1.26	15.20	58,612,237	774,491	700,409	1,602,860	891,442	67,347
3H-4, 85-88	19.85	20.29	110.2	1.27	15.20	121,921,012	555,556	1,087,963	1,516,204	670,253	92,593
3H-4, 125-128	20.25	20.69	112.8	1.31	15.20	37,255,130	474,537	694,444	740,741	390,981	115,741
3H-5, 5-8	20.55	20.99	114.8	1.34	15.20	52,545,387	1,242,284	2,052,469	1,498,843	670,253	270,062
3H-5, 45-48	20.95	21.39	117.4	1.33	15.20	9,531,475	144,676	482,253	265,239	167,563	48,225
3H-5, 85-88	21.35	21.79	120.1	1.32	15.20	11,920,466	212,191	1,446,759	1,051,312	446,835	173,611
3H-5, 125-128	21.75	22.19	122.7	1.32	15.20	4,451,904	98,380	248,843	717,593	55,854	57,870
3H-6, 5-8	22.05	22.49	125.2	1.34	8.55	339,506	17,361	416,667	77,160	3,858	32,793
3H-6, 45-48	22.45	22.89	129.8	1.34	8.55	10,128,898	92,593	590,278	99,826	279,272	219,907
3H-6, 85-88	22.85	23.29	134.5	1.31	8.55	27,584,620	617,284	1,302,083	149,498	502,690	376,157
3H-6, 125-128	23.25	23.69	139.2	1.27	8.55	23,241,407	352,045	472,608	250,772	2,178,321	38,580
3H-7, 5-8	23.55	23.99	142.7	1.29	8.55	45,335,237	702,160	1,512,346	729,167	2,681,011	297,068
4H-2, 5-8	23.99	24.43	147.9	1.21	8.55	85,205,503	1,282,793	1,822,917	1,323,302	893,670	445,602
4H-2, 43-45	25.55	25.99	166.1	1.24	8.55	35,300,406	378,086	499,614	985,725	251,345	209,298
4H-2, 85-88	25.93	26.37	170.5	1.26	8.55	89,187,103	987,654	1,095,679	1,990,741	726,107	462,963
4H-2, 125-128	26.35	26.79	175.5	1.28	8.55	10,359,698	49,190	144,676	81,019	55,854	107,060
4H-3, 5-8	26.75	27.19	180.1	1.29	8.55	35,401,195	594,136	1,633,873	148,534	1,619,777	418,596
4H-3, 43-45	27.43	27.87	188.1	1.28	8.55	7,616,749	66,551	231,481	46,296	223,418	156,250
4H-3, 85-88	27.85	28.29	193.0	1.25	10.43	37,254,288	771,605	896,991	260,417	1,843,195	298,997
4H-3, 125-128	28.25	28.69	196.8	1.25	10.43	38,974,437	706,019	694,444	601,852	1,954,904	231,481
4H-4, 5-8	28.55	28.99	199.7	1.23	10.43	62,402,680	648,148	941,358	1,041,667	1,899,049	262,346
4H-4, 43-45	28.93	29.37	203.4	1.25	10.43	26,261,938	391,590	580,633	479,360	5,138,604	54,012
4H-4, 85-88	29.35	29.79	207.4	1.26	10.43	49,787,651	1,201,775	1,120,756	1,161,265	2,681,011	256,559
4H-4, 125-128	29.75	30.19	211.2	1.27	10.43	37,640,484	981,427	663,310	595,625	783,921	135,369
4H-5, 5-8	30.05	30.49	214.1	1.27	10.43	37,683,754	787,037	501,543	540,123	865,743	185,185
4H-5, 45-48	30.45	30.89	217.5	1.25	13.33	39,534,144	601,852	516,975	493,827	1,298,615	208,333
4H-5, 85-88	30.85	31.29	220.5	1.27	13.33	72,032,653	391,590	499,614	337,577	55,854	310,571
4H-5, 1225-128	31.25	31.69	223.5	1.27	13.33	42,181,452	626,929	501,543	260,417	335,126	482,253
4H-6, 5-8	31.55	31.99	225.8	1.25	13.33	55,154,329	711,806	486,111	625,000	1,117,088	503,472
4H-6, 48-50	31.98	32.42	229.0	1.25	13.33	40,387,826	482,253	925,926	1,157,407	1,117,088	289,352
4H-6, 85-88	32.35	32.79	231.8	1.27	13.33	33,760,246	555,556	590,278	989,583	2,345,885	399,306
4H-6, 125-128	32.75	33.19	234.8	1.29	13.33	41,985,507	694,444	597,994	1,292,438	1,899,049	462,963
4H-7, 5-8	33.05	33.49	237.0	1.29	13.33	64,649,030	964,506	733,025	3,086,420	2,234,176	540,123
4H-7, 45-48	33.45	33.89	240.0	1.29	22.31	36,493,198	1,064,815	925,926	1,921,296	1,452,214	115,741
5H-1, 5-8	33.55	33.99	240.4	1.27	22.31	41,670,778	270,062	1,060,957	1,369,599	1,228,797	347,222
5H-1, 45-48	33.95	34.39	242.2	1.29	22.31	27,567,452	270,062	756,173	938,465	1,452,214	243,056
5H-1, 85-88	34.35	34.79	244.0	1.23	22.31	29,882,733	200,617	570,988	1,257,716	1,228,797	185,185
5H-1, 125-128	34.75	35.19	245.8	1.28	22.31	36,772,636	416,667	833,333	486,111	1,172,942	277,778

Table T2 (continued).

Core, section, interval (cm)	Depth (mbsf)	Depth (mcd)	Age (ka)	Density (g/cm3)	Sedimentation rate (cm/k.y.)	Marine diatoms (organisms/g dry sediment)	Silicoflagellates (organisms/g dry sediment)	Radiolarians (organisms/g dry sediment)	Freshwater diatoms (organisms/g dry sediment)	Chrysophyceans cysts (organisms/g dry sediment)	Phytoliths (organisms/g dry sediment)
5H-2, 5-8	35.05	35.49	247.2	1.28	22.31	44,899,106	366,512	1,060,957	2,189,429	1,452,214	443,673
5H-2, 45-48	35.45	35.89	249.0	1.18	22.31	76,391,166	324,074	763,889	486,111	2,010,758	208,333
5H-2, 85-88	35.85	36.29	250.8	1.27	22.31	15,808,770	135,031	434,028	115,741	893,670	347,222
5H-2, 125-128	36.25	36.69	252.6	1.16	22.31	32,994,697	127,315	520,833	81,019	1,061,233	231,481
5H-3, 5-8	36.55	36.99	253.9	1.28	22.31	32,940,230	193,385	541,477	541,477	1,903,809	348,092
5H-3, 43-45	36.93	37.37	255.6	1.15	22.31	41,309,666	193,385	367,431	212,723	1,903,809	96,692
5H-3, 85-88	37.35	37.79	257.5	1.26	22.31	86,906,876	347,222	833,333	1,064,815	3,462,972	555,556
5H-3, 125-128	37.75	38.19	259.3	1.16	22.31	65,268,212	96,451	462,963	308,642	2,457,593	192,901
5H-4, 5-8	38.05	38.49	260.6	1.28	22.31	71,760,777	277,778	771,605	1,087,963	3,127,846	354,938
5H-4, 45-48	38.45	38.89	262.4	1.21	22.31	47,565,531	135,031	405,093	607,639	446,835	154,321
5H-4, 85-88	38.85	39.29	264.2	1.29	22.31	58,759,661	632,716	324,074	455,247	1,452,214	262,346
5H-4, 125-128	39.25	39.69	266.0	1.26	20.12	51,809,667	1,280,864	493,827	2,291,667	2,010,758	493,827
5H-5, 5-8	39.55	39.99	267.5	1.24	20.12	104,774,511	1,574,074	679,012	2,376,543	1,899,049	478,395
5H-5, 43-45	39.93	40.37	269.4	1.24	20.12	84,768,266	729,167	270,062	877,701	446,835	135,031
5H-5, 85-88	40.35	40.79	271.5	1.22	20.12	55,370,868	462,963	254,630	439,815	781,962	277,778
5H-5, 125-128	40.75	41.19	273.5	1.25	20.12	63,617,246	462,963	231,481	270,062	1,787,341	366,512
5H-6, 5-8	41.05	41.49	274.9	1.29	20.12	50,852,639	439,815	462,963	439,815	1,899,049	185,185
5H-6, 45-48	41.45	41.89	276.9	1.23	20.12	101,724,822	810,185	729,167	1,620,370	1,340,505	189,043
5H-6, 85-88	41.85	42.29	278.9	1.19	20.12	52,293,422	740,741	578,704	439,815	1,340,505	138,889
5H-6, 125-128	42.25	42.69	280.9	1.20	20.12	84,979,508	810,185	567,130	945,216	2,904,429	162,037
5H-7, 5-8	42.55	42.99	282.4	0.99	20.12	77,033,464	837,191	432,099	1,336,806	2,234,176	432,099
5H-7, 45-48	42.95	43.39	284.4	1.24	20.12	99,262,200	1,053,241	526,620	326,003	2,792,720	275,849
6H-1, 5-8	43.05	46.37	299.20	1.26	20.12	108,437,140	406,108	966,923	1,218,324	1,791,820	232,062
6H-1, 125-128	44.25	47.57	305.16	1.30	20.12	111,214,234	648,148	787,037	1,782,407	2,345,885	162,037
6H-2, 85-88	45.35	48.67	310.63	1.26	20.12	74,939,153	350,205	431,021	457,960	1,560,023	323,266
6H-3, 65-68	46.65	49.97	317.09	1.28	20.12	99,733,670	270,062	189,043	769,676	781,962	54,012
6H-4, 25-28	47.75	51.07	322.55	1.30	20.76	44,134,648	208,333	393,519	717,593	3,909,808	46,296
6H-5, 5-8	49.05	52.37	329.01	1.33	20.76	54,889,272	243,056	675,154	1,728,395	1,675,632	54,012
6H-5, 125-1228	50.25	53.57	336.31	1.29	11.14	37,627,783	831,255	669,622	854,346	2,228,604	738,894
6H-6, 85-88	51.35	54.67	343.61	1.26	11.14	80,145,136	619,593	646,532	1,804,901	1,448,593	1,131,431
6H-7, 65-68	52.65	55.97	352.23	1.25	11.14	81,793,547	1,624,431	487,329	5,766,732	671,933	1,245,397
7H-1, 125-128	53.75	57.95	365.37	1.29	11.14	89,725,611	1,858,779	862,042	7,839,198	1,448,593	431,021
7H-2, 105-108	55.05	59.25	373.99	1.30	19.82	55,988,817	371,299	208,855	1,578,019	1,231,876	208,855
7H-4, 45-48	57.49	61.69	390.18	1.23	19.82	15,034,630	324,886	812,216	920,511	895,910	189,517
7H-5, 5-8	58.59	62.79	397.48	1.35	19.82	75,278,015	270,062	810,185	1,107,253	1,675,632	162,037
7H-5, 125-128	59.79	63.99	405.44	1.31	19.82	43,933,944	189,517	433,182	297,812	1,119,888	81,222
7H-6, 105-108	61.09	65.29	414.06	1.22	19.82	65,919,295	348,092	626,566	417,711	3,359,663	812,216
8H-1, 25-28	62.26	66.46	422.27	1.20	8.72	86,344,964	1,574,074	393,519	1,203,704	1,340,505	277,778
8H-1, 145-148	63.46	67.66	431.04	1.22	8.72	80,856,979	974,659	406,108	893,437	1,679,831	460,256
8H-2, 105-108	64.55	68.75	439.00	1.28	11.43	95,161,439	1,276,339	649,773	928,247	2,463,753	580,154
8H-3, 85-88	65.85	70.05	456.06	1.29	11.43	112,497,755	594,136	378,086	783,179	2,569,302	270,062

Table T3. Species compositon and related environmental preferences of the seven diatom groups, Site 1077.

Diatom group	Species composition (average %)	Environmental conditions
Freshwater	2.7	Related to the Congo River discharge
Aulacoseira spp.	64.0	
Marine	97.3	
Nearshore		
Low salinity	18.8	Related to the Congo River plume
Cyclotella litoralis		
High nutrients	64.0	
Chaetoceros spp	24.2	Highly productive waters where river-induced upwelling is inferred
Thalassionema nitzschioides var. *nitzschioides*	39.8	Highly productive nearshore waters to the north of the river plume nearshore
Neritic	11.0	
Actinocyclus aff. *curvatulus*		
Actinocyclus octonarius		
Coscinodiscus radiatus		
Rhizosolenia setigera/pungens		
Skeletonema costatum		
Thalassiosira angulata		
Thalassiosira eccentrica		
Littoral	0.7	Transported from the shelf
Actinoptychus senarius		
Actinoptychus vulgaris		
Offshore		
Warm	1.7	Related to the warm, high saline waters of the SECC with low nutrient levels
Alveus marinus		
Asteromphalus flabellatus		
Azpeitia nodulifera		
Nitzschia interruptestriata		
Planktoniella sol		
Pseudosolenia calcar-avis		
Rhizosolenia bergonii		
Thalassionema nitzschioides var. *parva*		
Thalassionema nitzschioides var. *inflatula*		
Thalassiosira ferelineata		
Thalassiosira lineata		
Thalassiosira simonsenii		
Oceanic temperate	3.2	Related to cold, nutrient-rich waters of the BCC, probably reflecting northward movement of the ABF
Bacteriastrum elongongatum/furcatum		
Fragilariopsis doliolus		
Thalassiosira oestrupii var. *oestrupii*		

Notes: Data are based on observations of van Iperen et al. (1987), Pokras and Molfino (1986), and Romero et al., (1999a). SECC = South Equatorial Countercurrent, BCC = Benguela Coastal Current, ABF = Angola Benguela Front.

Table T4. Concentrations of marine diatom groups, Site 1077. (See table note. Continued on next two pages).

Core, section, interval	Age (ka)	Neritic (valves/g dry sediment)	Littoral (valves/g dry sediment)	Warm (valves/g dry sediment)	Oceanic temperate (valves/g dry sediment)	High nutrients: *Chaetoceros* spp. RS (valves/g dry sediment)	High nutrients: *T. nitzschiolides* (valves/g dry sediment)	Low salinity (valves/g dry sediment)
175-1077B-								
1H-1, 5-8	0.3	4,098,550	360,788	1,664,435	67,347	10,551,842	8,858,702	8,580,126
1H-1, 45-48	2.5	3,999,807	401,235	1,128,472	463,927	12,103,303	12,399,676	6,814,236
1H-1, 85-88	4.8	3,081,621	174,667	873,334	212,095	10,734,204	14,672,199	4,779,580
1H-1, 125-128	7.0	2,213,542	225,694	529,514	243,056	9,048,412	5,808,857	2,345,885
1H-2, 5-8	8.8	3,863,826	417,711	730,994	382,902	14,533,573	8,287,168	3,023,697
1H-2, 45-48	10.6	7,123,395	923,617	1,246,883	554,170	16,184,493	8,580,126	6,574,383
1H-2, 85-88	12.5	3,693,648	522,139	870,231	183,715	8,101,868	21,165,876	503,949
1H-2, 125-128	14.3	3,502,047	336,735	894,754	384,840	6,488,227	11,310,167	3,677,197
1H-3, 5-8	16.1	2,233,188	177,115	1,047,288	577,549	6,807,878	31,216,029	10,881,016
1H-3, 45-48	17.9	5,871,491	376,205	1,679,488	403,077	12,452,789	37,680,875	48,907,330
1H-3, 85-88	19.7	2,989,969	289,352	607,639	154,321	8,354,126	11,729,423	14,745,560
1H-3, 125-128	22.6	2,888,720	326,301	690,989	652,601	54,625,143	77,029,045	29,566,704
1H-4, 5-8	24.8	2,353,395	192,901	569,059	192,901	9,655,181	30,384,791	20,554,417
1H-4, 45-48	27.0	9,467,310	202,041	952,480	481,050	5,977,170	75,326,824	43,569,213
1H-4, 85-88	29.2	3,337,191	163,966	540,123	327,932	24,670,091	33,400,928	19,102,203
175-1077A-								
2H-1, 45-46	29.4	8,721,650	415,777	937,916	1,286,008	11,019,361	14,054,589	28,053,185
2H-1, 85-86	31.6	10,146,605	231,481	790,895	1,813,272	10,836,622	19,102,203	51,777,024
2H-1, 125-126	33.8	11,612,654	250,772	713,735	6,587,577	10,691,235	12,399,676	40,271,018
2H-2, 5-6	35.5	4,542,607	409,009	1,018,170	11,330,409	24,962,937	9,183,078	41,155,870
2H-2, 45-46	37.7	4,652,778	381,944	963,542	9,192,708	17,391,137	17,147,299	36,640,483
2H-2, 85-86	39.9	2,595,486	121,528	642,361	3,203,125	18,642,560	6,702,527	23,123,719
2H-2, 125-126	42.1	5,204,004	380,992	1,030,410	4,589,221	15,708,679	9,192,993	27,188,972
2H-3, 5-6	43.8	21,976,237	1,403,973	2,889,167	7,135,895	38,903,516	11,422,854	28,109,179
2H-3, 45-46	46.0	4,268,842	519,534	961,139	4,286,160	28,959,080	14,541,643	19,054,566
2H-3, 85-86	48.2	3,689,780	313,283	461,223	1,705,653	19,311,285	10,862,910	8,343,163
2H-3, 125-126	50.2	4,281,537	313,283	713,590	1,801,378	16,934,555	8,399,157	7,447,253
2H-4, 5-6	51.7	5,330,039	317,493	1,250,731	2,366,768	33,203,917	9,638,713	9,861,574
2H-4, 45-46	53.7	3,886,960	250,772	694,444	2,266,590	35,566,877	17,929,261	16,700,464
2H-4, 85-86	55.7	6,052,941	290,077	1,005,600	1,624,431	36,235,299	11,142,882	13,494,646
175-1077B-								
2H-4, 104-105	57.5	2,592,593	162,037	1,053,241	3,750,000	23,663,147	8,322,305	19,381,475
2H-4, 144-145	59.5	4,977,816	225,694	1,128,472	4,689,429	24,407,224	17,314,862	446,835
2H-5, 35-36	61.6	6,705,843	240,525	1,260,352	5,762,985	24,258,192	23,957,496	222,860
2H-5, 75-76	63.6	7,990,248	275,161	1,471,052	7,535,174	20,549,861	17,048,823	780,011
2H-5, 115-116	65.6	4,024,884	125,386	802,469	1,592,400	11,086,524	8,043,033	670,253
2H-6, 4-5	67.5	5,918,210	476,466	727,238	1,956,019	14,016,030	11,338,442	670,253
2H-6, 44-45	69.6	3,347,801	451,389	1,103,395	1,918,403	17,841,483	15,862,648	1,508,069
2H-6, 84-85	71.6	5,228,056	175,102	1,175,687	1,225,717	8,607,412	8,134,406	222,860
175-1077C-								
3H-1, 105-106	73.6	825,753	11,603	133,435	114,097	3,247,674	3,247,674	1,119,888
3H-1, 145-146	75.6	1,349,825	11,603	175,980	212,723	2,127,786	4,927,505	895,910
175-1077A-								
3H-1, 48-50	79.0	2,970,679	135,031	723,380	501,543	5,156,313	5,585,439	6,255,692
3H-1, 85-88	81.3	2,977,109	122,171	752,315	1,118,827	8,999,949	12,213,494	24,873,824
3H-1, 128-130	84.0	8,574,460	283,565	1,026,235	850,694	21,324,093	14,968,978	27,815,488
3H-2, 5-8	85.8	11,913,580	740,741	1,944,444	2,314,815	24,170,114	16,532,901	96,516,393
3H-2, 45-48	88.3	4,835,519	188,572	727,348	1,212,247	15,310,007	5,682,941	19,723,148
3H-2, 85-88	90.8	8,344,907	351,080	999,228	2,349,537	30,723,569	7,372,780	17,203,153
3H-2, 125-128	93.3	2,459,491	48,225	453,318	559,414	8,361,320	4,356,643	3,016,137
3H-3, 5-8	95.2	8,198,302	424,383	983,796	2,121,914	23,137,554	11,170,879	18,767,077
3H-3, 45-48	97.7	3,084,496	67,347	552,246	956,328	9,143,397	5,237,220	5,794,371
3H-3, 85-88	100.3	7,048,611	702,160	1,215,278	2,214,506	14,453,394	9,830,373	35,746,812
3H-3, 125-128	102.9	3,969,907	297,068	742,670	675,154	2,775,533	2,345,885	5,473,731
3H-4, 5-8	104.9	10,964,506	607,639	1,350,309	1,485,340	11,525,643	5,920,566	39,991,746
3H-4, 48-48?	107.8	3,044,087	87,551	747,552	255,919	13,004,884	9,638,713	31,813,326
3H-4, 85-88	110.2	5,115,741	254,630	1,585,648	219,907	12,993,463	5,138,604	96,404,685
3H-4, 125-128	112.8	3,043,981	104,167	746,528	405,093	11,091,129	2,681,011	19,102,203
3H-5, 5-8	114.8	4,712,577	216,049	1,309,799	756,173	15,075,160	14,633,851	15,639,230
3H-5, 45-48	117.4	1,572,145	72,338	260,417	289,352	3,063,355	2,262,103	1,982,831
3H-5, 85-88	120.1	916,281	19,290	260,417	202,546	3,798,099	3,016,137	3,630,536
3H-5, 125-128	122.7	280,671	23,148	124,421	52,083	1,982,831	1,368,433	530,617

Table T4 (continued).

Core, section, interval	Age (ka)	Neritic (valves/g dry sediment)	Littoral (valves/g dry sediment)	Warm (valves/g dry sediment)	Oceanic temperate (valves/g dry sediment)	High nutrients: *Chaetoceros* spp. RS (valves/g dry sediment)	High nutrients: *T. nitzschiolides* (valves/g dry sediment)	Low salinity (valves/g dry sediment)
3H-6, 5-8	125.2	20,255	3,858	12,539	7,716	42,438	81,983	170,718
3H-6, 45-48	129.8	711,806	66,551	206,887	214,120	2,234,176	6,660,637	0
3H-6, 85-88	134.5	2,165,316	86,806	477,431	327,932	14,968,978	8,797,067	558,544
3H-6, 125-128	139.2	2,850,116	127,797	419,560	274,884	7,344,566	11,952,840	223,418
3H-7, 5-8	142.7	7,413,194	229,552	648,148	553,627	16,248,103	19,995,873	111,709
4H-2, 5-8	147.9	2,822,145	357,832	789,931	1,228,781	14,618,506	58,926,386	6,367,401
4H-2, 43-45	166.1	1,110,629	121,528	324,074	793,306	6,212,880	25,441,677	1,228,797
4H-2, 85-88	170.5	2,546,296	694,444	879,630	2,530,864	3,915,682	56,357,084	22,062,486
4H-2, 125-128	175.5	791,377	31,829	173,611	580,150	592,258	5,697,148	2,429,666
4H-3, 5-8	180.1	2,018,711	337,577	708,912	958,719	5,004,182	22,453,467	3,798,099
4H-3, 43-45	188.1	339,988	69,444	120,081	257,523	1,843,195	4,719,696	223,418
4H-3, 85-88	193.0	3,428,819	366,512	390,625	602,816	6,868,509	24,073,244	1,340,505
4H-3, 125-128	196.8	4,346,065	370,370	995,370	1,018,519	10,154,447	20,610,272	1,340,505
4H-4, 5-8	199.7	3,973,765	462,963	1,003,086	1,103,395	28,632,694	25,581,313	1,228,797
4H-4, 43-45	203.4	2,849,151	587,384	573,881	749,421	6,255,692	14,075,307	1,117,088
4H-4, 85-88	207.4	4,104,938	553,627	958,719	1,633,873	9,813,186	32,172,131	335,126
4H-4, 125-128	211.2	1,637,968	263,970	609,162	967,890	17,078,286	17,022,292	0
4H-5, 5-8	214.1	3,086,420	432,099	520,833	1,481,481	10,152,258	20,275,145	1,619,777
4H-5, 45-48	217.5	2,982,253	459,105	462,963	1,331,019	9,179,585	10,668,189	14,354,579
4H-5, 85-88	220.5	3,672,840	270,062	904,707	8,898,534	2,177,400	9,104,266	46,694,274
4H-5, 1225-128	223.5	2,734,375	376,157	1,147,762	9,823,495	951,541	5,082,750	21,448,087
4H-6, 5-8	225.8	5,434,028	520,833	1,979,167	11,319,444	6,662,540	9,606,956	18,711,222
4H-6, 48-50	229.0	14,795,525	607,639	1,485,340	1,938,657	7,511,843	12,399,676	1,340,505
4H-6, 85-88	231.8	4,192,708	538,194	902,778	1,284,722	6,593,095	19,381,475	502,690
4H-6, 125-128	234.8	8,622,685	694,444	1,263,503	1,755,401	10,077,113	18,543,659	893,670
4H-7, 5-8	237.0	10,204,475	771,605	1,977,238	1,861,497	12,669,737	36,417,065	670,253
4H-7, 45-48	240.0	9,409,722	451,389	706,019	983,796	7,195,659	15,862,648	1,675,632
5H-1, 5-8	240.4	6,008,873	279,707	569,059	1,215,278	6,814,236	16,086,066	10,388,917
5H-1, 45-48	242.2	3,564,815	364,583	452,353	560,378	4,718,775	14,522,143	3,127,846
5H-1, 85-88	244.0	3,888,889	270,062	578,704	347,222	5,392,886	14,745,560	4,412,497
5H-1, 125-128	245.8	3,883,102	277,778	520,833	549,769	7,602,246	16,086,066	7,540,343
5H-2, 5-8	247.2	5,970,293	289,352	752,315	1,138,117	5,458,472	16,197,774	14,745,560
5H-2, 45-48	249.0	5,983,796	266,204	729,167	682,870	9,060,508	36,975,609	22,230,049
5H-2, 85-88	250.8	2,121,914	96,451	236,304	260,417	2,900,831	8,210,596	1,731,486
5H-2, 125-128	252.6	4,641,204	347,222	248,843	468,750	2,492,316	17,538,280	6,702,527
5H-3, 5-8	253.9	6,903,834	212,723	415,777	502,800	6,105,408	13,662,629	4,479,550
5H-3, 43-45	255.6	7,590,349	125,700	464,123	454,454	5,487,449	23,517,640	2,799,719
5H-3, 85-88	257.5	5,462,963	277,778	636,574	1,354,167	9,117,856	51,274,334	18,320,241
5H-3, 125-128	259.3	3,269,676	221,836	318,287	356,867	8,829,026	44,571,807	7,372,780
5H-4, 5-8	260.6	6,226,852	246,914	378,086	671,296	7,746,835	48,034,779	7,931,324
5H-4, 45-48	262.4	2,826,003	115,741	356,867	424,383	4,580,060	34,685,579	4,133,225
5H-4, 85-88	264.2	1,728,395	61,728	331,790	648,148	6,590,819	42,225,922	6,925,945
5H-4, 125-128	266.0	1,666,667	246,914	841,049	1,782,407	4,753,498	39,656,620	2,569,302
5H-5, 5-8	267.5	3,657,407	246,914	632,716	2,060,185	4,607,240	90,037,284	3,239,555
5H-5, 43-45	269.4	21,132,330	189,043	378,086	850,694	2,399,897	56,301,230	3,462,972
5H-5, 85-88	271.5	7,997,685	462,963	428,241	520,833	3,992,842	35,523,395	6,143,983
5H-5, 125-128	273.5	7,320,602	212,191	376,157	626,929	5,716,438	33,624,345	14,968,978
5H-6, 5-8	274.9	7,141,204	231,481	335,648	682,870	4,225,818	28,709,159	9,271,829
5H-6, 45-48	276.9	8,912,037	108,025	580,633	891,204	12,453,688	57,753,444	20,107,582
5H-6, 85-88	278.9	9,120,370	277,778	451,389	844,907	6,641,147	26,698,401	7,819,615
5H-6, 125-128	280.9	12,287,809	378,086	378,086	1,188,272	9,633,962	42,337,631	18,208,533
5H-7, 5-8	282.4	11,329,090	445,602	621,142	985,725	13,959,914	30,943,334	18,208,533
5H-7, 45-48	284.4	11,460,262	200,617	589,313	752,315	11,594,914	42,896,175	31,166,752
6H-1, 5-8	299.20	9,350,150	541,477	928,247	406,108	16,358,443	60,921,886	19,486,044
6H-1, 125-128	305.16	24,803,241	717,593	729,167	1,412,037	7,604,262	57,753,444	17,314,862
6H-2, 85-88	310.63	6,977,156	552,246	660,001	0	7,208,675	38,443,424	20,558,874
6H-3, 65-68	317.09	11,072,531	648,148	904,707	1,242,284	11,059,170	48,816,741	25,693,021
6H-4, 25-28	322.55	7,025,463	439,815	590,278	1,550,926	19,437,329	13,516,763	1,273,148
6H-5, 5-8	329.01	17,500,000	297,068	1,147,762	378,086	12,677,105	21,671,505	893,670
6H-5, 125-1228	336.31	6,430,683	150,088	1,477,787	785,074	10,766,572	17,605,974	111,430
6H-6, 85-88	343.61	5,805,317	323,266	1,198,778	2,101,228	22,393,798	48,026,422	0
6H-7, 65-68	352.23	3,668,508	216,591	988,196	1,813,948	19,316,215	55,546,425	0
7H-1, 125-128	365.37	11,193,082	646,532	1,980,004	1,050,614	16,707,182	56,606,548	1,002,872
7H-2, 105-108	373.99	7,031,468	440,917	719,391	162,443	18,300,580	27,885,201	1,007,899
7H-4, 45-48	390.18	8,257,527	568,551	1,299,545	1,597,358	1,903,809	0	270,739
7H-5, 5-8	397.48	11,315,586	324,074	1,890,432	1,917,438	29,453,062	26,698,401	3,462,972

Table T4 (continued).

Core, section, interval	Age (ka)	Neritic (valves/g dry sediment)	Littoral (valves/g dry sediment)	Warm (valves/g dry sediment)	Oceanic temperate (valves/g dry sediment)	High nutrients: *Chaetoceros* spp. RS (valves/g dry sediment)	High nutrients: *T. nitzschiolides* (valves/g dry sediment)	Low salinity (valves/g dry sediment)
7H-5, 125-128	405.44	5,116,959	446,719	920,511	1,597,358	15,477,829	20,157,977	0
7H-6, 105-108	414.06	2,332,219	92,825	545,345	2,065,349	25,421,449	34,940,493	335,966
8H-1, 25-28	422.27	6,979,167	312,500	543,981	2,337,963	22,073,087	53,843,636	185,185
8H-1, 145-148	431.04	5,834,416	433,182	744,531	2,274,204	21,869,796	49,051,077	514,403
8H-2, 105-108	439.00	10,674,835	278,474	777,406	1,786,875	31,067,299	50,506,931	0
8H-3, 85-88	456.06	4,064,429	189,043	540,123	22,604,167	23,224,376	61,551,543	0

Note: RS = resting spores.